Author Responses to Referees and comments on

Modeling organic aerosol over Europe in summer conditions with the VBS-GECKO parameterization: sensitivity to secondary organic compound properties and IVOC emissions

Victor Lannuque[1,2,3,a], Florian Couvidat[2], Marie Camredon[1], Bernard Aumont[1] and Bertrand Bessagnet[2,b]

[1] LISA, UMR CNRS 7583, IPSL, Université Paris Est Créteil and Université de Paris, 94010 Créteil Cedex, France.
[2] INERIS, National Institute for Industrial Environment and Risks, Parc Technologique ALATA, 60550 Verneuil-en-Halatte, France.
[3] Agence de l'Environnement et de la Maîtrise de l'Energie, 20 avenue du Grésillé - BP 90406, 49004 Angers Cedex 01, France.
[a] Now at: CEREA, Joint Laboratory École des Ponts ParisTech – EDF R & D, Université Paris-Est, 77455 Marne la Vallée, France.
[b] Now at: Laboratoire de Métérologie Dynamique, IPSL, CNRS, UMR8539, 91128 Palaiseau Cedex, France.

Correspondence to: Victor Lannuque (victor.lannuque@lisa.u-pec.fr.com) and Florian Couvidat (florian.couvidat@ineris.fr)

We thank the reviewers for their comments on the manuscript. We outline below responses to the points raised by each referee and summarize the changes made to the revised manuscript.

Reponses to Referee 1

> *The results of the study are definitely relevant for the scientific community but still it will be interesting to discuss what happen when model configuration considers simultaneous the changes of two or more parameterization properties and also combinations between the IVOC emissions from vehicle exhausts and the parameterization properties.*

Sensitivity tests were run to (1) test the robustness of the VBS-GECKO parameterization to the uncertainties of the VBS-GECKO species properties and (2) quantify the sensitivity of the model results to IVOC emissions. Due to the high computation cost of these simulations, it was necessary to limit the number of sensitivity tests. The

objectives (1) and (2) are dissociated here and the sensitivity tests on each VBS-GECKO parameterization property and IVOC emission configuration were therefore run separately. Results on objective (1) show that the uncertainties in some parameter values of the VBS parameterization have a limited impact on the formation of SOA, and that therefore the parameterization is robust enough for 3D applications. Running tests simultaneously would be of important calculation costs and would not bring additional information on the robustness of the parameterization.

> *Specific comments: Pg. 6, Line 19 I suggest to rephrase "ECMWF in the EURODELTA-III project was shown to be one of the most representative models over Europe." in a meaningful way since ECMWF is not a model.*

You are right. Here "ECMWF" is related to IFS (Integrated Forecasting System) model from ECMWF. "ECMWF" has been replaced by "ECMWF-IFS" in the manuscript.

Reponses to Referee 2

> *1. POA and SVOC: Throughout the manuscript, the use of the terms POA and SVOC is unclear. For example, on page 4, lines 21-24, the authors describe the SVOC/POA ratio used in this work. What does this mean? Are those the SVOCs in the gas-phase ratioed against the POA in the particle phase? If yes, how does the statement on line21, 'POA from emission inventories are considered as SVOC' make sense? Also, is the ratio used to just determine the SVOC emissions and that the POA and SVOC are then repartitioned in the model? Also, a more elaborate justification of the source-resolved SVOC/POA ratios is warranted. A sentence saying 'This factor was shown to give satisfactory results' is insufficient.*

In the manuscript, "POA" is always related to the primary organic aerosol provided in the emission inventory. This POA, originally considered as non-volatile, has been shown since the study by Robinson et al. (2007) to be a set of semi-volatile species. Here, "SVOC(s)" corresponds to this set of semi-volatile species. In this study, all emitted POA were treated as SVOCs according the Robinson et al. (2007) volatility distribution and fraction (SVOC/POA ratio equal to 1, see Figure 11). Depending on their volatility, these SVOCs partition in the model between the gas and the particle.

The term "SVOC/POA ratio" is indeed not clear in the manuscript, as it has been used to modify the emission fluxes. The term "SVOC/POA ratio" was removed in the revised version of the manuscript and the sentences "a SVOC/POA ratio of 5 is used assuming that wood burning emissions are underestimated (e.g. Denier Van Der Gon et al., 2015). This factor was shown to give satisfactory results on OA estimations (Couvidat et al. 2012, 2018)." were changed into "POA emitted from residential wood burning have been shown to be significantly underestimated over Europe (e.g. Denier Van Der Gon et al., 2015). In this study, POA emissions from residential sources have therefore been increased by a factor of 5 as advised by Couvidat et al. (2012, 2018)."

> 2. POA: How is the POA dealt with in VBS-GECKO or is the POA formulation borrowed from H2O? If yes, I am a little concerned that the POA volatility distribution used in this work relies on that reported in Robinson et al. (2007). The Robinson parameterization is from a small off-road diesel engine and is probably not very representative of the gasoline- and diesel-powered sources in Europe. There has been significant amount of experimental (e.g., May et al., 2013a,b,c, Louvaris et al., 2017) and modeling (e.g.,Woody et al., 2016, Jathar et al., 2017; Akherati et al., 2019) work since the Robinson paper in parameterizing and applying the POA volatility by source. While I would like to see these parameterizations be used in the base simulations, at the very least, insight from earlier work needs to be included as a sensitivity study to show the influence of source-resolved POA volatility on regional OA mass concentrations.

Significant amount of experimental and modeling studies has indeed been published on SVOC and IVOC emissions since the Robinson et al. (2007) paper. The reference to these studies are now included in the revised version of the manuscript.

The purpose of this paper is the implementation and the evaluation of the VBS-GECKO parameterization in a CTM. The reference simulations were performed with the latest published version of H^2O (Couvidat et al., 2018) that uses the SVOC distribution of POA emissions from Robinson et al. (2007). This POA treatment was thus kept unchanged in this study. Possible errors in the simulated OA mass can indeed be due to the use of the Robinson et al. (2007) to represent the volatility distribution of POA emitted by all activity sectors. A discussion on this has been added in the conclusion of the manuscript.

For the evaluation of the VBS-GECKO parameterization (sections 3 and 4), the emitted POA distribution into S/IVOC volatility bins, as well as the gaseous oxidation chemical mechanisms for these S/IVOCs, are thus the same than in the latest published version of the H^2O (Couvidat et al., 2018), used here as a reference. For the study of OA sensitivity on IVOC emissions using the VBS-GECKO parameterization (section 5), the POA

distribution into S/IVOC volatility bins is different for traffic sources (SNAP 7 and 8). This new distribution of POA emissions still follows the volatility distribution provided by Robinson et al. (2007), but using the VBS-GECKO species to fill 9 volatility bins (i.e. linear n-alkane and 1-alkene species (C14 to C26) as shown in Figure 11), and the VBS-GECKO parameterization to represent the gaseous oxidation chemical mechanism of these S/IVOCs.

> *3. VBS-GECKO parameterization: The description for the OA model is incomplete (confusing at times) and needs to be significantly improved.*

Most of these questionings deals with the architecture, the optimization and the evaluation of the VBS-GECKO parameterization. These points are described in detail in a previous paper (Lannuque et al., 2018). It appears however from this comment that not enough information on the VBS-GECKO parameterization is provided in this manuscript. The section describing the VBS-GECKO parameterization was therefore modified to include additional information on its structure and its relationship with the GECKO-A explicit mechanisms (section 2.2.2). Specific answers to the referee comments are provided below.

> *Here are a few examples to help restructure this section:*
(i) How are IVOCs dealt with and what surrogates are used to model their SOA formation?
(ii) How are IVOC emissions developed?
(iii) Does this section describe the treatment of SVOCs too and if yes, what surrogates are used? I am concerned that the manuscript treats SVOCs and IVOCs interchangeably.

The VBS-GECKO parameterization is a VBS type parameterization that represents the formation of SOA from a set of defined primary species: aromatic compounds (benzene, toluene, and o- m- and p-xylenes), biogenic compounds (α-pinene, β-pinene and limonene), linear n-alkanes (tetradecane, octadecane, docosane, hexacosane) and linear 1-alkenes (tetradecene, octadecene, docosene, hexacosene).

In this study, SOA formation from NMVOC emissions was taken into account for mono-aromatic compounds, terpenes and long carbon chain NMVOCs. These long carbon chain NMVOCs have a carbon number lower or equal to 13 (organic compounds having a carbon number greater or equal to 14 being not included in NMVOC emission inventories as their vapor pressure fall in the IVOC range). α-pinene, β-pinene and limonene VBS-

GECKO precursors were used as surrogate species to represent the terpenes. Benzene, toluene, and o- m- and p-xylene VBS-GECKO precursors were used to represent the mono-aromatic compounds, and the C10 and C14 linear n-alkanes and 1-alkenes to represent the long carbon chain NMVOCs.

SVOC emission factors were taken into account considering the volatility distribution provided by Robinson et al. (2007). In section 3 and 4, this volatility distribution was filled up using the 3 precursors present in the H^2O parameterization, having saturation vapor pressures at 298 K of 8.9×10^{-11}, 8.4×10^{-9} and 3.2×10^{-7} atm respectively In sections 5, the SVOC volatility distribution was filled up using the VBS-GECKO precursors, i.e. with a mixing of C18, C22 and C26 linear n-alkanes and 1-alkenes (see Figure 11).

IVOC emissions were not considered in section 3 and 4. In section 5, IVOC emission factors were taken into account considering the volatility distribution of inferred IVOCs provided by Robinson et al. (2007). the IVOC volatility distribution was filled up using the VBS-GECKO precursors, i.e. with a mixing of C14 and C18 linear n-alkanes and 1-alkenes (see Figure 11).

(iv) How is the NOx dependence modeled? I am guessing that the ratios that are being talked about discuss the branching ratio between RO2 and NO and RO2 and HO2. Are there separate VBSs for products formed at different NOx levels? How are species formed at a high (low) NOx level then aged or transformed when they react further at a low (high) NOx level? All of these have implications on how results in the sensitivity section (4.3) are interpreted.

The stoichiometric coefficients of the VBS-GECKO parameterization (called $a_{k,RRR,i}$, where k is the precursor and i the number of the volatility bin) are NOx dependent. This NOx dependence is represented according to fraction of RO_2 reacting with NO, called the RRR ratio, calculated as:

$$RRR = \frac{k_{RO_2+NO}[NO]}{k_{RO_2+NO}[NO]+k_{RO_2+HO_2}[HO_2]}$$

where k_{RO2+NO} and $k_{RO2+HO2}$ are the rate constants for the reactions of the peroxy radicals with NO (set to 9.0×10^{-12} cm^3 $molec^{-1}$ s^{-1} according Jenkin et al., 1997 at 298 K) and with HO_2 (set to 2.2×10^{-11} cm^3 $molec^{-1}$ s^{-1} according to Boyd et al., 2003, assuming a large carbon skeleton for RO_2 at 298 K), respectively. Each stoichiometric coefficient has 5 tabulated values corresponding to RRRs of 0, 0.1, 0.5, 0.9 and 1. The entire range of NOx conditions is covered by a linear interpolation of the coefficients between the two tabulated RRR values

that encompass the calculated RRR. The formed $VB_{k,i}$ for the precursor k and the volatility bin i are not dependent on level of NOx. More details on the NOx dependence of the stoichiometric coefficients were added to the revised version.

(v) It is unclear whether each precursor gets a separate 7-bin VBS. Does it? If yes, the properties of the VBS bins remain the same but the mass yields are different?

Yes. In the VBS-GECKO parameterization, each precursor k has its own set of (1) 7 volatility bins, called $VB_{k,i}$ where i is the bin number, (2) 35 stoichiometric coefficients $a_{k,RRR,i}$, for the formation of the $VB_{k,i}$ during the gaseous reaction of the precursor with OH, plus 35 stoichiometric coefficients $b_{k,RRR,i}$ if the precursor k reacts also with O_3, and 35 stoichiometric coefficients $c_{k,RRR,i}$ if the precursor k reacts with NO_3, (3) 210 stoichiometric coefficients $d_{k,RRR,i,j}$ for the formation of the $VB_{k,j}$ during the gaseous reaction with OH of the 6 more volatile $VB_{k,i}$ and (4) 1 factor ϕ_k for the photolysis in the gas phase of the 6 more volatile $VB_{k,i}$. The properties of each $VB_{k,i}$ (i.e. molar weights (Mw), saturation vapor pressures (P^{sat}) at 298 K, effective Henry's law constants (H^{eff}) at 298K and vaporizations enthalpies (ΔH_{vap})) are the same for all precursor. The structure of the VBS-GECKO parameterization was added to the manuscript.

(vi) How is partitioning modeled for a given species between the organic and aqueous phases? Presumably, aqueous refers to the water associated with inorganic aerosol. Also, what about water uptake by the organic species itself?

The gas/aerosol partitioning of the precursors and VBk,i from the VBS-GECKO was taken into account for species having a low volatility, using the Raoult's law and considering an equilibrium between the gas phase and an organic aerosol phase. In the section dealing with the sensitivity tests on the hydro-solubility of organic compounds (section 4.1), the gas/aerosol partitioning was taken into account for species having a low volatility and also a high solubility, using the Raoult's and the Henry's law respectively, and considering the equilibrium between the gas phase, an organic aerosol phase and an aqueous aerosol phase. The gas/aerosol partitioning was calculated in this study using the SOAP thermodynamic module (Couvidat and Sartelet, 2015). These details were added to the revised version.

The influence of organic species on the aerosol hygroscopicity was not taken into account in this study.

(vii) How are the saturation vapor pressures (Psat) for the VBS species determined? The Psat values are changed in the sensitivity simulations. A change in the Psat values by an order of magnitude should dramatically change the SOA produced. Wouldn't this affect the evaluation of GECKO predictions against chamber or flow reactor measurements? In fact, an evaluation of GECKO predictions was not discussed at all. Again, these have implications on how results in the sensitivity section (4.4) are interpreted. Finally, I think I understand very generally how GECKO is used to determine the mass yields and properties of the VBS product species but since this is the main contribution of this work, it would be better to provide a paragraph length description of how this is done and what those parameterizations represent.

The GECKO-A chemical mechanisms were evaluated in several publications by comparisons with chamber experiments (e.g. Valorso et al., 2011; Denjean et al., 2015; La et al., 2016; McVay et al., 2016) and field campaign measurements (e.g. Lee-Taylor et al., 2011, 2015; Hodzic et al., 2013). The evaluation of GECKO-A chemical mechanisms is largely out of the scope of this study.

The development and the evaluation of the VBS-GECKO parameterization on the basis of GECKO-A explicit chemical mechanisms was the purpose of the Lannuque et al. (2018) paper. This paper describes in particular (1) the optimization of the VBS-GECKO parameters on a learning set of GECKO-A explicit simulations and (2) the evaluation of the VBS-GECKO parameterization by comparison with a validation set of GECKO-A explicit simulations. As mentioned above, the section describing the VBS-GECKO parameterization was modified in order to improve the understanding.

In this work, sensitivity tests were performed on the VBS-GECKO parameterization, and not on the GECKO-A explicit chemical mechanisms. In the GECKO-A tool, the physico-chemical properties of organic species (such as Psat298K) are estimated using structure-activity relationships (SAR). Comparisons between different SARs have shown that estimated Psat can vary by more than one order of magnitude (Valorso et al., 2011). The mandatory use of SAR in GECKO-A necessarily induces uncertainties, which affects the VBS-GECKO parameterization. The sensitivity tests on Psat are therefore performed to estimate the impact of this uncertainties on OA mass.

In the VBS-GECKO parameterization, the saturation vapor pressures (P^{sat}) of the $VB_{k,i}$ are fixed values at 298 K (see Table 1). The number of volatility bins and the values of the P^{sat} of each bin were determined during the development of the parameterization and are presented in Lannuque et al. (2018). I quote Lannuque et al. (2018): "Tests were performed to establish the best number and range of volatility bins to get a compromise between the reliability and the size of the VBS-GECKO parameterization. The partitioning of organic species having a Psat298K lower than 10^{-12} atm is almost exclusively in the particulate phase under typical atmospheric conditions. Therefore, the lower volatility bin in the VBS-GECKO parameterization lumps all species having a P^{sat}_{298K} lower than $10^{-12.5}$ atm. Similarly, organic species having a P^{sat}_{298K} above 10^{-6} atm are dominantly in the gas phase under typical atmospheric conditions and volatility bin is included for species having a P^{sat}_{298K} above $10^{-5.5}$ atm. Between these thresholds, the gas/particle partitioning of a species depends sensitively on temperature and OA load, so that a finer volatility discretization is desirable. A total of 7 volatility bins were selected for the VBS-GECKO parameterization. The boundaries of the k volatility bins i, $VB_{k,i}$, are the same for all the precursors k. Bin intervals at 298 K are shown in Table 2 and in Figure 5 (of Lannuque et al., 2018) by the different colours of the SOC bubbles. The properties of the k volatility bins i, $VB_{k,i}$, are set to the same value for the various precursors k. Each of the $VB_{k,i}$ has for assigned saturation vapour pressure the central value of its logarithmic interval".

> *4. Sensitivity simulations for ageing: I have major concerns in how the sensitivity simulations were performed and the interpretation drawn from the model predictions. Perhaps, some of these concerns stem from a lack of transparency in how the VBS-GECKO parameterizations were developed and how ageing was modeled. For example, if the VBS-GECKO parameterizations are constrained to predictions from GECKO, which already includes ageing, why are another set of ageing reactions modeled in CHIMERE? In fact, how is ageing defined? Is it defined as the transformation past the time period, the GECKO simulations were run for?*

In the VBS-type parameterizations, the term "aging" is generally associated with all the reactions impacting secondary organic species, and leading to functionalization, fragmentation and/or oligomerization of the organic matter. Here, the term "aging" is therefore associated with the "$VB_{k,i}$ + OH" and "$VB_{k,i}$ + hv" gaseous reactions, for i equal 1 to 6. This aging is indeed implicitly included in GECKO-A chemical mechanisms, and is considered in the architecture of the VBS-GECKO parameterization with stoichiometric coefficients for the formed $VB_{k,j}$, (for j equal 1 to 7) optimized on the basis of GECKO-A simulations (Lannuque et al., 2018). No additional set of aging reactions were considered in the VBS-GECKO-A parameterization for its use in CHIMERE. A sentence

was added to the manuscript to define the term "aging". The description of the VBS-GECKO parameterization structure in the revised version will also help in clarifying how the aging is represented.

> *Also, if there is a need to model additional ageing, what is the justification for such a high kOH? Is this kOH value constrained? If yes, against what laboratory or field data?*

In the VBS-GECKO parameterization, a k_{OH} of 4.10^{-11} cm^3 molec^{-1} s^{-1} is used for all the $VB_{k,i}$, for i equal 1 to 6. This value is in the upper range of the k_{OH} values estimated for the secondary organic compounds explicitly simulated with GECKO-A (see Lannuque et al., 2018). In the building of the VBS-GECKO parameterization, this k_{OH} value is first fixed, and then stoichiometric coefficients are optimized. A high value of k_{OH} for the reactivity of a $VB_{k,i}$ + OH is thus compensated by lower values of stoichiometric coefficients related to the formation of the $VB_{k,j}$ (with j different from i) and a higher value of the coefficient related to the reformation of the $VB_{k,j}$. In the manuscript, sensitivity tests were performed on this k_{OH} value to indirectly evaluate the stability of the VBS-GECKO parameterization to the uncertainty in the simulated OH concentrations.

> *How is ageing modeled in VBS-GECKO? Does it use the 'bulldozer' mechanism of Robinson et al. (2007)? There is evidence that this type of ageing mechanism may overestimate SOA production in regional models (e.g., refer to Lane et al. (2008) for biogenic SOA and Jathar et al. (2016) for all SOA) and might require explicit modeling of fragmentation reactions (Shrivastava et al., 2013; 2015).*

For each precursor k, the gaseous fraction of the $VB_{k,i}$ (for i equal 1 to 6) reacts with OH to form the corresponding 7 $VB_{k,j}$ (for j equal 1 to 6) (see Table S2 and Lannuque et al., 2018). By definition, the volatility of the $VB_{k,i}$ decreases as i increases. Thus in the VBS-GECKO parameterization, the reaction of the $VB_{k,i}$ with OH considers both fragmentation and functionalization pathways, the formation of a $VB_{k,j}$ with j < i being associated with fragmentation and the formation of a $VB_{k,j}$ with j > i being associated with functionalization. Unlike the mechanism of Robinson et al. (2007), fragmentation is therefore taken into account. To improve the manuscript clarity, the terms "fragmentation" and "functionalization" are now mentioned in the description of VBS-GECKO.

> *Finally, the conclusion that 'aging rates are likely not a major source of uncertainty' needs to be framed in context of how it is modeled in this work and findings from earlier work.*

You are right. This conclusion is related to the sensitivity tests performed in this study on the k_{OH} value of the VBS-GECKO papameterization. It is now mentioned in the text.

> *5. IVOC simulations: I am not sure how varying the IVOC fraction of NMVOC represents a changing fleet. Presumably, the NMVOC emissions as part of the inventory already represent a fixed fraction of gasoline versus diesel sources. A changing fleet (e.g., more diesel and less gasoline) would reduce the total NMVOC emissions from mobile sources since diesels emit less NMVOC than gasoline per mile driven. So, a higher IVOC fraction could still result in a lower IVOC emission. Either this is part has not been described well or the emissions simulations are not accounting for changing total NMVOC emissions with a changing fleet.*

You are right. Sensitivity tests were performed on total IVOC emissions. IVOC emissions were estimated as 150% of POA emissions (Robinson et al., 2007), and 4, 16, 30 or 65% of NMVOC emissions (Zhao et al., 2015, 2016). The term "fleet change" is thus not the right term. This was modified in the abstract, in the introduction, in section 5 and in the conclusion.

> *Also, it needs to be stated that these emissions are only being applied to mobile sources and also only to tailpipe emissions (i.e., not evaporative emissions). Is that right?*

The sensitivity tests on IVOC emissions were performed on all "road transport" emissions (SNAP 7) and all "other mobile source and machinery" emissions (SNAP 8). SNAP 7 includes tailpipe emissions but also "evaporation of gasoline from vehicles" which are thus both considered in our study (SNAP 7 also includes emissions due to abrasion of tires and brake pads and to road wear which are negligible in term of organic compound emissions). These precisions were added to the revised version.

> *6. Grammar and style: There are numerous grammatical mistakes in the manuscript and the style could be improved too to enhance readability.*

The manuscript has been re-read and corrected to try to enhance readability.

Minor comments:
> *1. Page 2, lines 5-9: Can this first paragraph include newer citations when discussing OA and SOA?*

Recent citations were added to the introduction of the revised version of the manuscript.

> 2. Page 2, line 19: The SOA in chamber experiments rarely represents oxidation products after a single oxidation step. Rephrase.

The sentence was not about SOA in chamber experiments but about the Odum approach. This sentence was anyway removed from the manuscript as this paragraph was modified to take into account the next comment.

> 3. Page 2, paragraph starting on line 16: This could benefit from reviewing the literature on a few other types of SOA modeling. For example, Jathar et al.'s (GMD, 2015) use of the statistical oxidation model. Or Li et al.'s (AE, 2015) use of the master chemical mechanism. In other words, there aren't just two approaches to model SOA but rather several methods that span a continuum in complexity.

As suggested by the referee, the paragraph was modified to list the various types of SOA parameterizations for 3D applications. The use of the MCM chemical scheme in CTMs was not added here as this approach is still rarely applied because of important calculation costs.

> 4. Page 4, line 10: Is the particle size resolution too low to separate PM1 from PM2.5? Wouldn't numerical diffusion add uncertainty to how PM is split in that 1 to 2.5µm region?

The size resolution of particles in the model allows thus to separate PM_1 and $PM_{2.5}$ (9 size bins from 10 nm to 10 µm with especially fixed cut off at 1 µm and 2.5 µm). The particular matter is distributed into these bins depending to its origin (biogenic, anthropogenic, dust, etc). The two sizes are used in the study as the available in-situ data are OM in PM_1 (ACSM) and OC in $PM_{2.5}$.

> 5. Page 4, line 22: The extensive emissions work done with open burning suggests that residential burning should have a lower SVOC/POA ratio than other anthropogenic combustion sources.

The term "SVOC/POA ratio" was unclear and removed in the revised version of the manuscript (see reply to general comment #1).

> *6. Section 2.2.2: To clarify, each precursor species in Table 1 gets a separate 7-binVBS?*

Exactly. For a better understanding, the volatility bins are now called $VB_{k,i}$, where k is the precursor and i the bin number (see reply to general comment #3.v).

> *7. Page 5, line 16: Rephrase 'VBS-GECKO considers the formation of 7 volatility bins'.*

It was replaced by: "In the VBS-GECKO parameterization, secondary organic species formed during the oxidation of a given precursor k are lumped into 7 volatility bins."

> *8. Page 5, line 28: How is RRR calculated in CHIMERE?*

RRR is the fraction of RO_2 reacting with NO (assuming that RO_2+RO_2 can be considered as negligible as done by Lane et al., 2008). RRR is calculated in each box at each chemical time step following the formula provided in the answer to the general comment #3.iv). This information was added to the manuscript.

> *9. Page 6, line 24: evaluated 'by' comparing.*

The text was modified.

> *10. Page 6, lines 24-32: Is there a reason for sub-selecting 7 stations for comparing the time series. What not do comparison at all available sites? Can details about how the OA is measured (e.g., filter followed by OC/EC, AMS) added to this paragraph?*

A total of 48 rural background stations was available for the comparison. The evaluation of the model was shown in the article using statistical indicators calculated on these 48 rural stations. Most of these stations provide $PM_{2.5}$ measurement and/or only few measurement points on the studied temporal period. All the stations were thus not of interest for temporal evolution comparisons of the aerosol organic fraction. Only stations providing OM_{PM1} and $OC_{PM2.5}$ measurements with a large amount of data on the studied period were selected. Measurements of OC

are performed by calcinations of filters and OM_{PM1} using an ACSM. This information was added to the manuscript.

> *11. Page 7, line 14: Please comment on whether regulatory agencies use the Boylan and Russell (2006) criteria when evaluating model output. My sense is that they do not.*

Regulatory agencies do not use the Boylan and Russell critera. It is still a criterion which has been used in different studies to evaluate the model performances (e.g. Couvidat et al., 2018; Lecœur and Seigneur, 2013; Jiang et al., 2019 ACPD; Ciarelli et al., 2017; Mircea et al., 2019). The references were added to the revised version.

> *12. Page 7, lines 20-25: What is the primary reason for differences in the ref versus VBS-GECKO simulations for OA mass concentrations (e.g., source treatment, chemistry)? It is important to discuss this since the VBS-GECKO leads to slightly better model performance.*

The purpose of the comparison between the H^2O and GECKO-VBS mechanism for SOA formation is to evaluate the reliability of the VBS-GECKO parameterization. The simulations performed with CHIMERE were therefore set up using the same configuration of the model (meteorological data, emissions, deposition, inorganic and organic gaseous chemical mechanism, inorganic and organic gas/particle partitioning…), but implementing either the H^2O or the GECKO-VBS parameterization for SOA formation. The implementation a given parameterization for SOA formation induces anyway some differences depending on the primary compounds considered and/or the processes taken into account in the parameterization. Here, the differences between the H^2O and VBS-GECKO in reference simulations come from the representation of:

(1) the secondary organic compounds that partition to form SOA. The H^2O parameterization is built to represent SOA formation from the condensation of hydrophobic species and hydrophilic species. In the reference H^2O simulation, the hydrophobic species were considered to condense only on an organic phase (depending on their saturation vapor pressure) and the hydrophilic species considered to condense both, on an organic phase and on an aqueous phase (depending on their Henry's constant). The VBS-GECKO parameterization is built to represent SOA formation from the condensation of species having a low volatility. In the simulation performed with the VBS-GECKO parameterization, the species were considered to condense on an organic phase only (depending on their saturation vapor pressure). The

differences between the two representations come from the consideration of SOA formation from the condensation of species with a high hydro-solubility in the H_2O parameterization, processes which is not included in the VBS-GECKO parameterization. Even if in the sensitivity test on the hydro-solubility (Section 4.1), the species were considered to condense both on an organic phase and an aqueous phase, the VBS-GECKO was not developed for this purpose (see response to minor comments #15).

(2) The ideality of the condensed phase. In the H^2O reference (i.e. the one evaluated by Couvidat et al., 2018), the organic and aqueous phases of the particle are considered as non-ideal, with estimations of activity coefficients. In the VBS-GECKO simulations, the particles were considered as ideal because of the difficulty to provide any estimation for activity coefficients.

(3) the SOA formation from emitted C_{10} to C_{13} precursors (from NMVOC inventory). These SOA precursors, included in the VBS-GECKO parameterization but not in the H^2O parameterization, are only considered when simulations are performed with the VBS-GECKO parameterization. The contribution of C_{10} to C_{13} precursors to the OA mass has however been shown to be very low and do not explain the differences between the H_2O and VBS-GECKO results.

The difference between the H^2O and VBS-GECKO results, and the slightly better model performances calculated with the VBS-GECKO parameterization, are thus expected to come dominantly from the parameterization used, as well as point (1) and (2) to represent SOA formation. A paragraph was added in section 2.2 of the revised version to better introduce the differences between the H^2O and VBS-GECKO reference simulations.

> 13. Page 7, line 30: Is this the Pearson r? If yes, please use the small letter 'r'? If not, please specific what correlation coefficient this is. Can you comment on the value of r? How does it compare to r from earlier regional modeling work (e.g., Ahmadov et al., JGR, 2012; Baker et al., ACP, 2015; Murphy et al., ACP, 2017)? It would be good to contrast the model skill across different geographical regions (i.e., United States versus Europe). To me an r2 of 0.25 doesn't sound that good. Does it?

This is the Pearson r. "R" was replaced by "r" in the text.

For CTM/measurement comparisons, standard r values are low notably because of the large number of data, variations and phenomena to be taken into account as meteorology and air mass transportation. Our r values (0.79 for OM and 0.58 for OC) are in the standard. For example, in the article by Akherati et al. (2019) that you quote, the 6 calculated r values on OM are between 0.11 and 0.56. The other quoted references give r values between 0.55 and 0.7 for OM (Murphy et al., 2017) or between 0.55 and 0.76 for OC (Ahmadhov et al., 2012) in USA.

Bergström et al. (2012) found r values around 0.6 for OM at a station in Switzerland. Ciarelli et al. (2017) calculated r values at different stations in Europe and highlight that the lower correlations are found in mountainous area, suggesting a likely important impact of modeled dynamics of air masses on this statistical value, more than the chemistry. Text was modified and references added.

> *14. Figure 3: It would improve interpretation of the data if the site location was specified in the panel instead of using the station number?*

It was modified in the text and the Figures.

> *15. Page 9, line 8: I thought a VBS species could condense in both the organic and aqueous phases depending on the organic and aqueous partitioning coefficients respectively. If not, how is this treatment in the reference model handled? Perhaps, there is a need for a table that talks about the different model configurations?*

The VBS-GECKO parameterization, as most of the one-dimension VBS parameterization types, was built to represents SOA formation from the partitioning onto an organic aerosol phase of organic compounds having a low volatility. A Henry's law constant was added to each volatility bin species to calculate their deposition. This parameter can also be used to represent their condensation onto an aqueous phase. However, the VBS-GECKO parameterization (1) does not include the major precursors of SOA formation from the condensation of hydro-soluble species and (2) was not optimised to represent this process. The VBS-GECKO reference simulation considers thus SOA formation from the condensation of organic species having a low volatility only. A test was performed Section 4.1 to evaluate the sensitivity of the model to the condensation of these organic species on an aqueous phase depending on their Henry's law constant. The text was modified to clarify this point.

> *16. Page 9, line 24: Where is Benelux? Is this location significant? If yes, please specify. Please also do so anywhere else results form a specific location are discussed.*

Benelux means "Belgium-Netherland-Luxembourg". It is now clarified in the text.

> 17. Figure 5: General comment: Given the very small differences in panels (a) and (d), at what percent level would one be able to say with confidence that there were differences in model predictions? In other words, what is the precision in the model?

All the simulations were carried out with the same inputs and on the same numerical environment. Moreover, CHIMERE use numbers in double precision. Simulation tests are regularly performed with CHIMERE, were also performed here. The differences observed here are because of the use of the different parameterizations.

> 18. Section 4.1: The results presented in this section are sensitive to the amount of aerosol water available? How well is aerosol water modeled when compared to measurements? In fact, how well is inorganic aerosol modeled when compared to measurements?

Yes, the results presented Section 4.1 on the OA sensitivity to the hydro-solubility of organic species are indeed influenced by the amount of water available in the aerosol. However, in the model configuration, the condensation of the VBS-GECKO species on the aqueous phase does not impact the inorganic nor the water content of aerosol. The comparison is therefore coherent.

Water and inorganic composition of aerosols are calculated with ISORROPIA which is widely used in air quality models. The evaluation of inorganics in CHIMERE for the simulated period was studied in details in Couvidat et al. (2018). It was not possible to evaluate the amount of water during this period due to the absence of measurements. However, Guo et al. (2015) estimated over southeastern USA that amounts of water calculated with ISORROPIA were in good agreement with measured liquid water based on differences in ambient and dry light scattering coefficients and Bougiatioti et al. (2016) show similar results over eastern Mediterranean.

> 19. Page 9, line 33: What does 'slightly' mean? Can you be quantitative?

Statistical values were incorporated into the text to be more quantitative.

> 20. Page 11, line 4: What does 'free NOx' mean?

"free NOx" was replaced by "remote NOx conditions" in the manuscript.

> *21. Page 11, line 5: What does 'whatever' mean?*

The entire range of RRR ratio (from remote to high NOx conditions) is covered over Europe in every model configuration. Text was modified.

> *22. Page 12, line 21: I am not sure why IVOCs would ever be in the particle phase. In the hot exhaust, IVOCs are likely to be in the vapor phase. When hot exhaust is diluted and cooled, the IVOCs probably don't have enough time to condense and then evaporate.*

You are right, it is a mistake. The sentence was removed from the text.

> *23. Page 13, lines 1-13: Are the IVOCs described here referred to as SVOCs in the lines following this section (lines 14-31)? This was quite confusing.*

The text was modified to be more understandable and to be clear on what treatments are apply to SVOCs (distribution in low volatility bins from Robinson et al. (2007) corresponding to C18, C22 and C26 in VBS-GECKO parameterization), to IVOCs (relative distribution in intermediate volatility bins from Robinson et al. (2007) corresponding to C14 and C18 in VBS-GECKO parameterization, and absolute flux of emission depending on model configuration) or both S/IVOCs (considered as 25% alkenes and 75% alkanes). **IVOC$_{150POA}$**, **IVOC$_{4VOC}$**, **IVOC$_{16VOC}$**, **IVOC$_{30VOC}$** and **IVOC$_{65VOC}$** are the names of the different tested configurations. I suppose a part of the confusion also came from the use of the "SVOC/POA ratio" which was modified in the manuscript.

> *24. Page 13, lines 14-31: I was hoping this would be covered in the methods section.*

Several sensitivity tests were performed on the parameterization properties and IVOC emissions. For clarity, the choice was made to describe the model configuration used for the sensitivity tests in each of the sensitivity test sections. We still think that it improves the clarity of the manuscript and this was not changed in the revised version. A sentence was however added at the end of the VBS-GECKO parameterization description section (Section 2.2) to list all the sensitivity tests and send to the corresponding sensitivity test section. "Changes were then applied to this configuration to perform sensitivity tests of SOA formation on secondary organic compound

properties (solubility, reactivity with OH, NOx/HO$_2$ condition dependency and volatility) or SVOC and IVOC (S/IVOC) emissions. For a better readability, the details of these modifications are presented for each test before results in section 4 (properties) and section 5 (S/IVOC emissions)."

> *25. Figure 14: Could these also include the measurements?*

The Figure shows the temporal evolution of the total OA mass concentrations by sources. Measurements at the stations provide only OM in PM$_1$ (from ACSM), OC in PM$_{2.5}$ (from filter calcinations) or PM$_{2.5}$. The model/measurement comparison on the total OA mass is thus not possible.

> *26. Page 15, lines 15-21: Are newly discovered pathways for SOA from autooxidation reactions and acid-catalyzed pathways included? If not, could these be cited here to provide context?*

These pathways are not considered in GECKO-A, and so neither in the VBS-GECKO which is developed based on GECKO-A simulations. These recently identified processes can indeed influence SOA formation. These processes are currently not included in the VBS-GECKO parameterization, and could possibly explain the discrepancies between model and measurements. Sentences were added to the conclusion of the manuscript to discuss the possible origin of the model/measure discrepancies, and suggest some future development to improve the reliability of SOA parameterizations.

> *27. Page 17, line 6: I do not recollect where the volatility of the OA was discussed and how the authors conclude that LVOC and ELVOC make up most of the OA*

The volatility of OA is discussed based on Figure 10 in Section 4.4 and based on Figure S2 in the last paragraph of Section 6. The terms "LVOC" and "ELVOC" were indeed not defined in the text and were thus removed in the revised manuscript.

References

Ahmadov, R., McKeen, S. A., Robinson, A. L., Bahreini, R., Middlebrook, A. M., de Gouw, J. A., Meagher, J., Hsie, E.-Y., Edgerton, E., Shaw, S. and Trainer, M.: A volatility basis set model for summertime secondary

organic aerosols over the eastern United States in 2006, J. Geophys. Res. Atmos., 117(D6), n/a-n/a, doi:10.1029/2011jd016831, 2012.

Akherati, A., Cappa, C. D., Kleeman, M. J., Docherty, K. S., Jimenez, J. L., Griffith, S. M., Dusanter, S., Stevens, P. S. and Jathar, S. H.: Simulating secondary organic aerosol in a regional air quality model using the statistical oxidation model - Part 3: Assessing the influence of semi-volatile and intermediate-volatility organic compounds and NOx, Atmos. Chem. Phys., 19(7), 4561–4594, doi:10.5194/acp-19-4561-2019, 2019.

Bergström, R., Denier Van Der Gon, H. A. C., Prévôt, A. S. H., Yttri, K. E. and Simpson, D.: Modelling of organic aerosols over Europe (2002-2007) using a volatility basis set (VBS) framework: Application of different assumptions regarding the formation of secondary organic aerosol, Atmos. Chem. Phys., 12(18), 8499–8527, doi:10.5194/acp-12-8499-2012, 2012.

Bougiatioti, A., Nikolaou, P., Stavroulas, I, Kouvarakis, G., Weber, R., Nenes, A., Kanakidou, M. and Mihalopoulos, N.: Particle water and pH in the eastern Mediterranean: Source variability and implications for nutrient availability, Atmos. Chem. Phys., 16(7), 4579–4591, doi:10.5194/acp-16-4579-2016, 2016.

Boyd, A. A., Flaud, P. M., Daugey, N. and Lesclaux, R.: Rate constants for RO2 + HO2 reactions measured under a large excess of HO2, J. Phys. Chem. A, 107(6), 818–821, doi:10.1021/jp026581r, 2003.

Ciarelli, G., Aksoyoglu, S., El Haddad, I., Bruns, E. A., Crippa, M., Poulain, L., Äijälä, M., Carbone, S., Freney, E., O'Dowd, C., Baltensperger, U. and Prévôt, A. S. H.: Modelling winter organic aerosol at the European scale with CAMx: Evaluation and source apportionment with a VBS parameterization based on novel wood burning smog chamber experiments, Atmos. Chem. Phys., 17(12), 7653–7669, doi:10.5194/acp-17-7653-2017, 2017.

Couvidat, F. and Sartelet, K.: The Secondary Organic Aerosol Processor (SOAP v1.0) model: a unified model with different ranges of complexity based on the molecular surrogate approach, Geosci. Model Dev., 8(4), 1111–1138, doi:10.5194/gmd-8-1111-2015, 2015.

Couvidat, F., Debry, É., Sartelet, K. and Seigneur, C.: A hydrophilic/hydrophobic organic (H2O) aerosol model: Development, evaluation and sensitivity analysis, J. Geophys. Res., 117(D10), D10304, doi:10.1029/2011JD017214, 2012.

Couvidat, F., Bessagnet, B., Garcia-Vivanco, M., Real, E., Menut, L. and Colette, A.: Development of an inorganic and organic aerosol model (CHIMERE 2017β v1.0): seasonal and spatial evaluation over Europe, Geosci. Model Dev., 11(1), 165–194, doi:10.5194/gmd-11-165-2018, 2018.

Denier Van Der Gon, H. A. C., Bergström, R., Fountoukis, C., Johansson, C., Pandis, S. N., Simpson, D. and Visschedijk, A. J. H.: Particulate emissions from residential wood combustion in Europe - revised estimates and an evaluation, Atmos. Chem. Phys., 15(11), 6503–6519, doi:10.5194/acp-15-6503-2015, 2015.

Denjean, C., Formenti, P., Picquet-Varrault, B., Camredon, M., Pangui, E., Zapf, P., Katrib, Y., Giorio, C., Tapparo, A., Temime-Roussel, B., Monod, A., Aumont, B. and Doussin, J. F.: Aging of secondary organic aerosol generated from the ozonolysis of α-pinene: Effects of ozone, light and temperature, Atmos. Chem. Phys., 15(2), 883–897, doi:10.5194/acp-15-883-2015, 2015.

Guo, H., Xu, L., Bougiatioti, A., Cerully, K. M., Capps, S. L., Hite, J. R., Carlton, A. G., Lee, S. H., Bergin, M. H., Ng, N. L., Nenes, A. and Weber, R. J.: Fine-particle water and pH in the southeastern United States, Atmos. Chem. Phys., 15(9), 5211–5228, doi:10.5194/acp-15-5211-2015, 2015.

Hodzic, A., Madronich, S., Aumont, B., Lee-Taylor, J., Karl, T., Camredon, M. and Mouchel-Vallon, C.: Limited influence of dry deposition of semivolatile organic vapors on secondary organic aerosol formation in the urban plume, Geophys. Res. Lett., 40(12), 3302–3307, doi:10.1002/grl.50611, 2013.

Jenkin, M. E., Saunders, S. M. and Pilling, M. J.: The tropospheric degradation of volatile organic compounds: a protocol for mechanism development, Atmos. Environ., 31(1), 81–104, doi:10.1016/S1352-2310(96)00105-7, 1997.

La, Y. S., Camredon, M., Ziemann, P. J., Valorso, R., Matsunaga, A., Lannuque, V., Lee-Taylor, J., Hodzic, A., Madronich, S. and Aumont, B.: Impact of chamber wall loss of gaseous organic compounds on secondary organic aerosol formation: Explicit modeling of SOA formation from alkane and alkene oxidation, Atmos. Chem. Phys., 16(3), 1417–1431, doi:10.5194/acp-16-1417-2016, 2016.

Lane, T. E., Donahue, N. M. and Pandis, S. N.: Simulating secondary organic aerosol formation using the volatility basis-set approach in a chemical transport model, Atmos. Environ., 42(32), 7439–7451, doi:10.1016/j.atmosenv.2008.06.026, 2008.

Lannuque, V., Camredon, M., Couvidat, F., Hodzic, A., Valorso, R., Madronich, S., Bessagnet, B. and Aumont, B.: Exploration of the influence of environmental conditions on secondary organic aerosol formation and organic species properties using explicit simulations: development of the VBS-GECKO parameterization, Atmos. Chem. Phys., 18(18), 13411–13428, doi:10.5194/acp-18-13411-2018, 2018.

Lecœur, E. and Seigneur, C.: Dynamic evaluation of a multi-year model simulation of particulate matter concentrations over Europe, Atmos. Chem. Phys., 13(8), 4319–4337, doi:10.5194/acp-13-4319-2013, 2013.

Lee-Taylor, J., Madronich, S., Aumont, B., Baker, A., Camredon, M., Hodzic, A., Tyndall, G. S., Apel, E. and Zaveri, R. A.: Explicit modeling of organic chemistry and secondary organic aerosol partitioning for Mexico City and its outflow plume, Atmos. Chem. Phys., 11(24), 13219–13241, doi:10.5194/acp-11-13219-2011, 2011.

Lee-Taylor, J., Hodzic, A., Madronich, S., Aumont, B., Camredon, M. and Valorso, R.: Multiday production of condensing organic aerosol mass in urban and forest outflow, Atmos. Chem. Phys., 15(2), 595–615, doi:10.5194/acp-15-595-2015, 2015.

McVay, R. C., Zhang, X., Aumont, B., Valorso, R., Camredon, M., La, Y. S., Wennberg, P. O. and Seinfeld, J. H.: SOA formation from the photooxidation of α-pinene: Systematic exploration of the simulation of chamber data, Atmos. Chem. Phys., 16(5), 2785–2802, doi:10.5194/acp-16-2785-2016, 2016.

Mircea, M., Bessagnet, B., D'Isidoro, M., Pirovano, G., Aksoyoglu, S., Ciarelli, G., Tsyro, S., Manders, A., Bieser, J., Stern, R., Vivanco, M. G., Cuvelier, C., Aas, W., Prévôt, A. S. H., Aulinger, A., Briganti, G., Calori, G., Cappelletti, A., Colette, A., Couvidat, F., Fagerli, H., Finardi, S., Kranenburg, R., Rouïl, L., Silibello, C., Spindler, G., Poulain, L., Herrmann, H., Jimenez, J. L., Day, D. A., Tiitta, P. and Carbone, S.:

EURODELTA III exercise: An evaluation of air quality models' capacity to reproduce the carbonaceous aerosol, Atmos. Environ. X, 2(March 2018), 100018, doi:10.1016/j.aeaoa.2019.100018, 2019.

Murphy, B. N., Woody, M. C., Jimenez, J. L., Carlton, A. M. G., Hayes, P. L., Liu, S., Ng, N. L., Russell, L. M., Setyan, A., Xu, L., Young, J., Zaveri, R. A., Zhang, Q. and Pye, H. O. T.: Semivolatile POA and parameterized total combustion SOA in CMAQv5.2: Impacts on source strength and partitioning, Atmos. Chem. Phys., 17(18), 11107–11133, doi:10.5194/acp-17-11107-2017, 2017.

Robinson, A. L., Donahue, N. M., Shrivastava, M. K., Weitkamp, E. A., Sage, A. M., Grieshop, A. P., Lane, T. E., Pierce, J. R. and Pandis, S. N.: Rethinking Organic Aerosols: Semivolatile Emissions and Photochemical Aging, Science (80-.)., 315(5816), 1259–1262, doi:10.1126/science.1133061, 2007.

Valorso, R., Aumont, B., Camredon, M., Raventos-Duran, T., Mouchel-Vallon, C., Ng, N. L., Seinfeld, J. H., Lee-Taylor, J. and Madronich, S.: Explicit modelling of SOA formation from α-pinene photooxidation: Sensitivity to vapour pressure estimation, Atmos. Chem. Phys., 11(14), 6895–6910, doi:10.5194/acp-11-6895-2011, 2011.

Zhao, Y., Nguyen, N. T., Presto, A. A., Hennigan, C. J., May, A. A. and Robinson, A. L.: Intermediate Volatility Organic Compound Emissions from On-Road Diesel Vehicles: Chemical Composition, Emission Factors, and Estimated Secondary Organic Aerosol Production, Environ. Sci. Technol., 49(19), 11516–11526, doi:10.1021/acs.est.5b02841, 2015.

Zhao, Y., Nguyen, N. T., Presto, A. A., Hennigan, C. J., May, A. A. and Robinson, A. L.: Intermediate Volatility Organic Compound Emissions from On-Road Gasoline Vehicles and Small Off-Road Gasoline Engines, Environ. Sci. Technol., 50(8), 4554–4563, doi:10.1021/acs.est.5b06247, 2016.

Modeling organic aerosol over Europe in summer conditions with the VBS-GECKO parameterization: sensitivity to secondary organic compound properties and IVOC emissions

Victor Lannuque[1,2,3,a], Florian Couvidat[2], Marie Camredon[1], Bernard Aumont[1] and Bertrand Bessagnet[2,b]

[1] LISA, UMR CNRS 7583, IPSL, Université Paris Est Créteil and Université de Paris, 94010 Créteil Cedex, France.
[2] INERIS, National Institute for Industrial Environment and Risks, Parc Technologique ALATA, 60550 Verneuil-en-Halatte, France.
[3] Agence de l'Environnement et de la Maîtrise de l'Energie, 20 avenue du Grésillé - BP 90406, 49004 Angers Cedex 01, France.
[a] Now at: CEREA, Joint Laboratory École des Ponts ParisTech – EDF R&D, Université Paris-Est, 77455 Marne la Vallée, France.
[b] Now at: Laboratoire de Métérologie Dynamique, IPSL, CNRS, UMR8539, 91128 Palaiseau Cedex, France.

Correspondence to: Victor Lannuque (victor.lannuque@lisa.u-pec.fr) and Florian Couvidat (florian.couvidat@ineris.fr)

Abstract. The VBS-GECKO parameterization for secondary organic aerosol (SOA) formation was integrated in the chemistry-transport model CHIMERE. Concentrations of organic aerosol (OA) and SOA were simulated over Europe for the July-August 2013 period. Simulated concentrations with the VBS-GECKO were compared to results obtained with the former H^{2}O parameterization implemented in CHIMERE and to observations from EMEP, ACTRIS and other observations available in the EBAS database. The model configuration using the VBS-GECKO parameterization slightly improves the performances compared to the model configuration using the former H^{2}O parameterization. The VBS-GECKO model configuration performs well for stations showing a large SOA concentration from biogenic sources, especially in northern Europe, but underestimates OA concentrations over stations close to urban areas. Simulated OA was found to be mainly secondary (~85%) and from terpene oxidation. Simulations show negligible contribution of the oxidation of mono-aromatic compounds to SOA production. Tests performed to examine the sensitivity of simulated OA concentrations to hydro-solubility, volatility, aging rates and NO$_x$ regime have shown that the VBS-GECKO parameterization provides consistent results, with a weak sensitivity to changes in the parameters provided by the gas phase mechanism included in CHIMERE (e.g. HO$_x$ or NO$_x$ concentrations). Different scenarios considering intermediate-volatility organic compound (IVOC) emissions were tested to examine the contribution of IVOC oxidation to SOA production. At the continental scale, these simulations show a weak sensitivity of OA concentrations to IVOC emission variations. At the local scale, accounting for IVOC emissions was found to lead to a substantial increase of OA concentrations in the plume from urban areas. This additional OA source remains too small to explain the gap between simulated and measured values at stations where anthropogenic sources are dominant.

1. Introduction

For the past 20 years, fine particulate matter or PM$_{2.5}$ (particles with a diameter smaller than 2.5 μm) has been regulated due to their health impacts and the resulting costs (e.g. Lim et al., 2012; WHO Regional Office for Europe and OECD, 2015).

5 Furthermore, fine particles degrade visibility (e.g. Han et al., 2012) and influence climate change (e.g. Boucher et al., 2013). Organic aerosol (OA) represents a large fraction of the total fine particle mass (e.g. Jimenez et al., 2009). This OA is either primary (directly emitted into the atmosphere) or secondary (formed by gas/particle partitioning of low volatile and/or highly soluble species produced during the oxidation of gaseous organic compounds) (e.g. Carlton et al., 2009; Kroll and Seinfeld, 2008). The secondary organic aerosol (SOA) dominates the primary organic aerosol (POA) in most environments (e.g.

10 Gelencsér et al., 2007; Jimenez et al., 2009).

Chemistry-transport models (CTMs) are used to investigate and identify air quality regulation policies. Parameterizations are developed and used in CTMs to represent SOA formation. Different approaches have been followed to describe SOA formation as the two-product model (e.g. Odum et al., 1996; Schell et al., 2001), the molecular approach (e.g. Pun et al., 2002, 2003), the volatility basis set (VBS) approach (e.g. Donahue et al., 2006, 2012) or the statistical oxidation model

15 (SOM) (e.g. Cappa and Wilson, 2012; Jathar et al., 2015). Parameterizations are constantly improved and additional processes were included in the parameterizations to improve the simulations of SOA concentrations, such as gas-phase aging of organic species (e.g. Rudich et al., 2007), more comprehensive emissions and multiphase chemistry. Robinson et al. (2007) have indeed shown that POA provided in emission inventories is in part composed of semi-volatile organic compounds (SVOCs) (existing both in particle and gas phases) and that a fraction of emitted organic compounds were

20 missing from these inventories: the intermediate-volatility organic compounds (IVOCs) (forming SOA after several oxidation stages) (e.g. Ots et al., 2016; Robinson et al., 2007; Woody et al., 2015). Numerous experimental and modeling studies have since explored the volatility distribution of SVOCs from POA emissions and of IVOC emissions depending on the emission source (e.g. Akherati et al., 2019; Grieshop et al., 2009; Hatch et al., 2018; Jathar et al., 2017; Louvaris et al., 2017; Lu et al., 2018; May et al., 2013a, 2013b, 2013c; Woody et al., 2016).

25 Other studies have highlighted the important role played by condensed phase processes in SOA formation, in particular the reactivity of hydrophilic products in the condensed phase (e.g. Couvidat et al., 2012; Couvidat and Seigneur, 2011; Knote et al., 2014; Paulot et al., 2009; Pun et al., 2006b; Surratt et al., 2010), the oligomerization of SVOCs in the aerosol (e.g. Aksoyoglu et al., 2011; Couvidat et al., 2012; Denkenberger et al., 2007; Dommen et al., 2006; Kalberer et al., 2006; Lemaire et al., 2016; Trump and Donahue, 2014), the non-ideal behavior of the organic aerosol (Couvidat et al., 2012,

30 Couvidat and Sartelet, 2015; Pun et al., 2006; Pye et al., 2018) or the effect of the aerosol viscosity (Couvidat and Sartelet, 2015; Shiraiwa et al., 2013). Comparisons with field observations have shown that CTMs using these parameterizations fall short to reproduce SOA concentration spatial and temporal variability (e.g. Aksoyoglu et al., 2011; Bessagnet et al., 2016;

Ciarelli et al., 2016; Couvidat et al., 2012; Heald et al., 2005; Im et al., 2015; Petetin et al., 2014; Pun et al., 2006a; Solazzo et al., 2012; Tsigaridis et al., 2014; Volkamer et al., 2006).

Most of these SOA parameterizations are optimized/built on the basis of atmospheric chamber data. Experiments are however limited in number and are usually performed under conditions that differ from the atmosphere. In addition, SOA

5 formation experiments can be subject to potential artefacts from chamber wall surfaces, such as aerosol and gaseous compound wall losses (e.g. La et al., 2016; Matsunaga and Ziemann, 2010; McMurry and Grosjean, 1985). Considering or not these artefacts for the parameterization development directly impact SOA representation in air quality models (e.g. Cappa et al. 2016).

The development of the VBS-GECKO parameterization explores another track using the results of an explicit model

10 representing the state of knowledge of organic gas-phase chemistry instead of atmospheric chamber data. The VBS-GECKO parameterization for SOA formation (Lannuque et al., 2018) is a VBS-type parameterization with gaseous aging. VBS-GECKO was optimized based on box modeling results using explicit oxidation mechanisms generated with the Generator for Explicit Chemistry and Kinetics of Organics in the Atmosphere (GECKO-A) modeling tool (Aumont et al, 2005; Camredon et al, 2007).

15 The objectives of this study are (i) to evaluate the behavior of the VBS-GECKO parameterization in the CTM CHIMERE (Menut et al., 2013, Mailler et al., 2017) by comparison with field measurements and previous simulations obtained with the H^2O parameterization (Couvidat et al., 2012) already implemented in CHIMERE, (ii) to explore the sensitivity of simulated SOA concentrations to organic compound properties (volatility, solubility, aging rates or NO_x regime) and (iii) to test the sensitivity of OA concentrations to the uncertainties on IVOC emission fluxes from traffic,. The setup of the CHIMERE

20 model and the implementation of the VBS-GECKO in the CTM are described in section 2. In section 3, the VBS-GECKO is evaluated over Europe for a two-month summer period, the sensitivity to organic compound properties is explored in section 4, and the sensitivity to the uncertainties in IVOC emission fluxes from traffic is investigated in section 5. Finally, results on simulated OA sources and concentrations are discussed in section 6.

2. Method

25 ### 2.1. The CHIMERE chemical transport model

The evaluation of the VBS-GECKO parameterization and the exploration of SOA sensitivity were performed using the CHIMERE 2017 β version. This version is based on the CHIMERE 2013 version (Menut et al., 2013) which was modified to improve the representation of particles with the implementation of a new aerosol module. Details of the CHIMERE 2017 β version and its evaluation are given in Couvidat et al. (2018).

30 Briefly, the CHIMERE 2017 β version uses the MELCHIOR2 gas-phase chemical scheme, involving 44 species reacting according to 120 reactions. MELCHIOR2 is a reduced version of the MELCHIOR1 mechanism, obtained by the Carter's surrogate molecule method (Carter, 1990). In CHIMERE, the aerosol evolution is described by a sectional aerosol module

(e.g. Bessagnet et al., 2004, 2009; Schmidt et al., 2001). The size distribution of aerosol particles is here represented using 9 bins, ranging from 10 nm to 10 μm. Aerosol formation is represented in the model by nucleation for sulfuric acid (Kulmala et al., 1998), coagulation between particles (e.g. Debry et al., 2007; Jacobson et al., 1994) and condensation/evaporation via absorption according to the "bulk equilibrium" approach (e.g. Pandis et al., 1993). For inorganic species, the gas/particle

5   equilibrium concentrations are calculated using the ISORROPIA v2.1 (Fountoukis and Nenes, 2007) thermodynamic module. For organic species, the equilibrium concentrations are calculated using the SOAP (Secondary Organic Aerosol Processor) thermodynamic module (Couvidat and Sartelet, 2015). The gaseous formation of secondary organic species able to partition between the gas and the condensed phases (so leading to SOA formation) are represented in the CHIMERE β version using the H^2O mechanism. Here, the VBS-GECKO parameterization was also implemented. The H^2O and VBS-

10   GECKO organic aerosol modules are described hereafter.

The chemical speciation of emitted non-methane volatile organic compounds (NMVOCs) is taken from Passant (2002) as described in Menut et al. (2013). POA from emission inventories are considered as SVOC. A factor 5 is apply to residential POA emissions, as wood burning emissions are underestimated in emission inventories (e.g. Denier Van Der Gon et al., 2015). This factor was shown to give satisfactory results on OA estimations (Couvidat et al. 2012, 2018). Biogenic emissions

15   are computed with the Model of Emissions and Gases and Aerosols from Nature MEGAN 2.1 algorithm (Guenther et al., 2012). Dry deposition for gaseous organic species is described using the Wesely (1989) parameterization and according to their Henry's law constants, as described by Bessagnet et al. (2010).

2.2. The organic aerosol modules

The purpose of the comparison between the H^2O and GECKO-VBS mechanisms for SOA formation is to evaluate the

20   reliability of the VBS-GECKO parameterization. The simulations performed with CHIMERE were therefore setup using the same configuration of the model (meteorological data, emissions, deposition, inorganic and organic gaseous chemical mechanism, inorganic and organic gas/particle partitioning…), but implementing either the H^2O or the GECKO-VBS parameterizations. The implementation of a given parameterization for SOA formation induces anyway some differences, related to the primary compounds considered and/or the processes taken into account in the parameterization. The

25   differences between the H^2O and VBS-GECKO are mentioned in the following parameterization presentation sections.

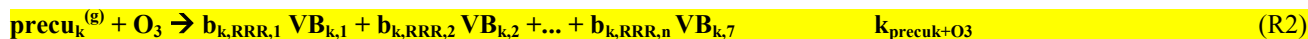### 2.2.1. The H^2O reference mechanism

The H^2O mechanism, described in details by Couvidat et al. (2018), considers SOA formation from the partitioning of hydrophilic species (condensing on an aqueous phase and an organic particulate phase) and hydrophobic species (condensing only on an organic particulate phase owing to their low affinity with water). Distinction between hydrophobic and

30   hydrophilic compounds is based on their octanol/water coefficient (Pun et al., 2006) or their partitioning between the organic and aqueous phases (Couvidat and Seigneur, 2011). H^2O considers the formation of hydrophilic and/or hydrophobic species from the gaseous oxidation of isoprene, monoterpenes (α-pinene, β-pinene, limonene and ocimene), sesquiterpenes

4

(humulene) and mono-aromatic precursors (toluene and xylenes). Note that in H$_2$O, limonene mechanism is used as a surrogate mechanism for ocimene (ocimene having its own OH, NO$_3$ and O$_3$ reaction rates). Each emitted SOA precursor is linked to a species of the H$_2$O mechanism. POA provided by emissions inventories are split into three emitted SVOCs having different volatilities (saturation vapor pressures at 298 K of 8.9×10^{-11}, 8.4×10^{-9} and 3.2×10^{-7} atm respectively) with a fraction that follows the volatility distribution of POA emissions given by Robinson et al. (2007). In H$_2$O, gaseous oxidation of these three compounds with OH leads to hydrophobic species with a lower volatility. No gaseous oxidation is considered for hydrophylic and hydrophobic species in H$_2$O. Activity coefficients for the H$_2$O species are computed with the thermodynamic model UNIFAC (UNIversal Functional group Activity Coefficient; Fredenslund et al., 1975). H$_2$O has been evaluated over Europe (Couvidat et al., 2012, 2018) and the Paris area (Couvidat et al., 2013; Zhu et al., 2016a, 2016b). The H$_2$O reference mechanism is presented in table S1 of supplementary material.

2.2.2. The VBS-GECKO parameterization

The VBS-GECKO parameterization is described in details in a previous paper by Lannuque et al. (2018). Briefly, VBS-GECKO is a volatility basis set (VBS) type parameterization that represents SOA formation from the partitioning of organic compounds having a low volatility onto an organic aerosol phase. The VBS-GECKO parameterization takes into account for the oxidation of a precursor k (precu$_k$) (1) the formation of 7 VB$_{k,i}$, where i is the number of the volatility bin (1 being the most volatile and 7 the less volatile) (reactions R1, R2 and R3), (2) the gas-phase ageing of the VB$_{k,i}$ (except for the lowest volatility bin 7) with OH redistributing the matter between the VB$_{k,i}$ (reactions R4) and by photolysis leading to a loss of carbon matter (reactions R4), (3) the gas/particle partitioning of the precursor k (R6) and of the VB$_{k,i}$ (R7) ; the VBS-GECKO follows this structure for a given precursor k:

$$\text{precu}_k^{(g)} + \text{OH} \rightarrow a_{k,RRR,1} \text{ VB}_{k,1} + a_{k,RRR,2} \text{ VB}_{k,2} + ... + a_{k,RRR,n} \text{ VB}_{k,7} \qquad k_{\text{precuk+OH}} \qquad (R1)$$

$$\text{precu}_k^{(g)} + \text{O}_3 \rightarrow b_{k,RRR,1} \text{ VB}_{k,1} + b_{k,RRR,2} \text{ VB}_{k,2} + ... + b_{k,RRR,n} \text{ VB}_{k,7} \qquad k_{\text{precuk+O3}} \qquad (R2)$$

$$\text{precu}_k^{(g)} + \text{NO}_3 \rightarrow c_{k,RRR,1} \text{ VB}_{k,1} + c_{k,RRR,2} \text{ VB}_{k,2} + ... + c_{k,RRR,n} \text{ VB}_{k,7} \qquad k_{\text{precuk+NO3}} \qquad (R3)$$

$$\text{VB}_{k,i}^{(g)} + \text{OH} \rightarrow d_{k,RRR,i,1} \text{ VB}_{k,1} + d_{k,RRR,i,2} \text{ VB}_{k,2} + ... + d_{k,RRR,i,n} \text{ VB}_{k,7} \qquad \forall i \neq 7 \quad k_{OH}=4.10^{-11} \text{cm}^3\text{molec}^{-1}\text{s}^{-1} \quad (R4)$$

$$\text{VB}_{k,i}^{(g)} + h\nu \rightarrow \text{ carbon lost} \qquad \forall i \neq 7 \quad \phi_k \text{ J}_{\text{acetone}} \qquad (R5)$$

$$\text{precu}_k^{(g)} \leftrightarrow \text{precu}_k^{(p)} \qquad (R6)$$

$$\text{VB}_{k,i}^{(g)} \leftrightarrow \text{VB}_{k,i}^{(p)} \qquad (R7)$$

In VBS-GECKO, the production and gaseous aging of the VB$_{k,i}$ for a precursor k are adjusted by stoichiometric coefficients ($a_{k,RRR,i}$, $b_{k,RRR,i}$, $c_{k,RRR,i}$, $d_{k,RRR,i}$, for reaction (R1) to (R4) respectively) which depend on NO$_x$ regime. The formation of more volatile and less volatile bins can be assimilated to fragmentation and functionalization processes, respectively. The stoichiometric coefficients depend on the NO$_x$ according to the reaction rate ratio (RRR) of RO$_2$ with NO:

$$RRR = \frac{k_{RO_2+NO}[NO]}{k_{RO_2+NO}[NO]+k_{RO_2+HO_2}[HO_2]} \qquad (1)$$

5

where k_{RO2+NO} (set to 9.0×10^{-12} cm^3 molec^{-1} s^{-1} according Jenkin et al., 1997 at 298 K) and $k_{RO2+HO2}$ (set to 2.2×10^{-11} cm^3 molec^{-1} s^{-1} according to Boyd et al., 2003, assuming a large carbon skeleton for RO$_2$ at 298 K) are the rate constants for the reactions of the peroxy radicals with NO, and HO$_2$ respectively and [NO] and [HO$_2$] the concentration of the radicals. The entire RRR range is covered by linear interpolation of the coefficients between the two closest values. The photolysis is considered as a limiting process for SOA formation, leading to a loss of matter. The photolysis rate of the VB$_{k,i}$ are based on the acetone one multiplied by an optimized factor ϕ_k, different for each precursor k. Precursors and VB$_{k,i}$ condense on an organic particulate phase according to an equilibrium between the gas and the organic particulate phase that follows the Raoult's law (reaction R6 and R7).

The properties of the 7 VB$_{k,i}$ were considered to be independent of the precursor k and set for each volatility bin i to the mean values simulated with explicit GECKO-A simulations. Table 1 gives the molar weights (Mw), saturation vapor pressures (P^{sat}) at 298 K, effective Henry's law constants (H^{eff}) at 298K and vaporizations enthalpies (ΔH_{vap}) used for each VB$_{k,i}$ VBS-GECKO species. The stoichiometric coefficients and factors ϕ_k were optimized on explicit GECKO-A simulations of gas-phase oxidation and SOA formation. The stoichiometric coefficients were optimized for 5 RRR values: 0, 0.1, 0.5, 0.9 and 1 (Lannuque et al., 2018). Precursors considered in the current VBS-GECKO parameterization are mono-aromatic compounds (benzene, toluene, and o- m- and p-xylenes) and n-alkanes (decane, tetradecane, octadecane, docosane and hexacosane) reacting with OH, and monoterpenes (α-pinene, β-pinene and limonene) and linear 1-alkenes (decene, tetradecene, octadecene, docosene and hexacosene) reacting with OH, O$_3$ and NO$_3$. Note that (1) the parameterization does not represent SOA formation from the partitioning of hydrophilic species, (2) recently indentified chemical processes such as autooxidation reactions or acid-catalyzed pathways, not include in GECKO-A, are thus not considered in the VBS-GECKO parameterization and (3) the high value of the reaction rate of the VB$_{k,i}$ ($k_{OH} = 4.10^{-11}$ cm^3 molec^{-1} s^{-1}) was fixed before optimization and is compensated by lower or higher values of optimized coefficients (see details in Lannuque et al., 2018). Tables of optimized stoichiometric coefficients are available in supplementary material of Lannuque et al. (2018).

For SOA production from NMVOC oxidation, the former H^{2}O parameterization in CHIMERE was replaced by the VBS-GECKO parameterization for terpenes and mono-aromatic compounds. The VBS-GECKO mechanisms were also implemented in CHIMERE for SOA formation from C10 to C13 alkanes and alkenes, gaseous species usually not considered in 3D models as SOA precursors. Each emitted SOA precursor not present in the VBS-GECKO was linked to a VBS-GECKO species. As in the H^{2}O mechanism, the VBS-GECKO parameterization for limonene was used as a surrogate mechanism for ocimene. The VBS-GECKO parameterizations for benzene, toluene, o-, m- and p-xylenes were also used as surrogate mechanisms for other emitted mono-aromatic compounds according to their SOA yield and reactivity with OH. n-dodecane and tetradecane VBS-GECKO species were used to lump emitted alkanes with 10 to 13 atoms of carbon, according to their carbon chain length. The VBS-GECKO mechanism for 1-decene was applied for all emitted C10 alkenes. The lumping scheme between emitted NMVOCs and VBS-GECKO species is given in Table 2. The current VBS-GECKO version does not represent SOA production from the oxidation of isoprene and sesquiterpenes. The H^{2}O parameterizations for isoprene and humulene were therefore left unchanged in CHIMERE to account for this SOA production. For SOA

6

production for SVOC oxidation distributed from POA emissions, the H^2O approach was kept unchanged (i.e. distribution of POA emissions into 3 SVOC species and representation of their SOA production using the H_2O mechanism). In CHIMERE, RRR is calculated in each box at each chemical time step following equation 1. Activity coefficients for the condensation of the VBS-GECKO species into the aerosol particulate phase are fixed to 1 (i.e. ideality of the organic particulate phase is considered). This implementation of the VBS-GECKO in CHIMERE was selected here as the reference configuration and is denoted ref-VBS-GECKO hereafter. The ref-VBS-GECKO mechanism is presented in table S2 of supplementary material and evaluated in section 3.

Changes were then applied to this reference configuration to perform sensitivity tests of SOA formation on secondary organic compound properties (solubility, reactivity with OH, NO_x/HO_2 condition dependency and volatility) or IVOC emission fluxes from traffic. For a better readability, the details of these modifications are presented for each sensitivity test in section 4 (properties) and section 5 (IVOC emissions).

2.3. Simulation setup and field measurements

The model was run to simulate the concentrations of OA over Europe (from 25° W to 45° E in longitude and from 30° to 70° N in latitude) with a horizontal resolution of 0.25° × 0.25° during the July-August 2013 period, SOA formation being expected to be important during summertime. Meteorology was obtained from Integrated Forecasting System (IFS) model of the European Centre for Medium-Range Weather Forecasts (ECMWF). This meteorology has been evaluated in Bessagnet et al. (2016) for the model intercomparison project EURODELTA-III. ECMWF-IFS in the EURODELTA-III project has been shown to be one of the most reliable models to represent meteorological conditions over Europe. Anthropogenic emissions of gases and particles were taken from the European Monitoring and Evaluation Programme (EMEP) inventory (methodology described in Vestreng, 2003) and boundary conditions were generated from the Model for OZone And Related Tracers (Mozart v4.0 (Emmons et al., 2010)). Wildfire emissions were not considered.

The VBS-GECKO mechanism was evaluated by comparing the simulated results to the H^2O mechanism and particulate phase measurements available in the EBAS database (http://ebas.nilu.no/). EBAS is a database hosting observation data of atmospheric chemical composition and physical properties in support of a number of national and international programs ranging from monitoring activities to research projects. EBAS is developed and operated by the Norwegian Institute for Air Research (NILU). This database is populated for example by the EMEP measurements (Tørseth et al., 2012) or the Aerosols, Clouds and Trace gases Research Infrastructure (ACTRIS, http://www.actris.eu/) ones. 48 rural background stations provide measurements for fine particulate matter and were thus selected here for a statistical evaluation: 36 stations for $PM_{2.5}$, 13 for $OC_{PM2.5}$ (organic carbon in $PM_{2.5}$, obtained by filter calcinations) and 6 for OM_{PM1} (organic matter in PM_1, obtained with ACSM). For the comparisons with OC measurements, the OM:OC ratio of the VBS-GECKO volatility bins were assumed to be equal to 1.8, in agreement with typical observed values given by Canagaratna et al. (2015). The location of the selected stations is shown in Fig. 1.a. Among these stations, 7 stations were used for time series comparisons:

7

- the Cabauw (NL0644R, Netherlands), Melpitz (DE0044R, Germany) and Palaiseau (FR0020R, SIRTA, France) rural background stations, located in areas dominantly impacted by anthropogenic air masses (see Figure S1 in supplementary material presenting the mean of the simulated ratios between toluene and α-pinene emission fluxes for the studied period).

- the Birkenes II (NO0002R, Norway), Diabla Gora (PL0005R, Poland), Hyytiälä (FI0050R, Finland) and Iskrba (SI0008R, Slovenia) rural background stations, located in areas dominantly impacted by biogenic emissions (see Figure S1 in supplementary material).

These 7 stations were selected among the 48 background station because the measurements at the station provide (1) a direct information on the organic fraction of fine particles, i.e. OM_{PM1} and $OC_{PM2.5}$ measurements, and (2) enough data over the studied period to perform time series comparisons .The location of the 7 selected stations is shown in Fig. 1.b.

Various statistical indicators were computed to evaluate the VBS-GECKO mechanism, including the Root Mean Square Error (RMSE), the correlation coefficient, the Mean Fractional Error (MFE) and the Mean Fractional Bias (MFB). MFB and MFE are calculated as:

$$MFB = \frac{1}{N}\sum_{i=1}^{N} \frac{\left(c_i^{mod} - c_i^{obs}\right)}{\left(\frac{c_i^{mod} + c_i^{obs}}{2}\right)},$$

(2)

$$MFE = \frac{1}{N}\sum_{i=1}^{N} \frac{\left|c_i^{mod} - c_i^{obs}\right|}{\left(\frac{c_i^{mod} + c_i^{obs}}{2}\right)},$$

(3)

where c_i^{mod} and c_i^{obs} are the simulated and observed concentrations of the studied component at the time i. and N the number of available in-situ measurement values. Boylan and Russell (2006) defined two criteria to evaluate the performances of a model. The model performance criteria (described as the level of accuracy that is considered to be acceptable for modeling applications) is reached when MFE ≤ 75% and |MFB| ≤ 50% whereas the performance goal (described as the level of accuracy that is considered to be close to the best values a model can be expected to achieve) is reached when MFE ≤ 50% and |MFB| ≤ 30%. These criteria are currently used to evaluate the reliability of the models (e.g. Ciarelli et al., 2017; Couvidat et al., 2018; Lecœur and Seigneur, 2013; Mircea et al., 2019).

3. Evaluation of the ref-VBS-GECKO parameterization

Figure 2.a shows the mean OA mass concentrations simulated with the ref-VBS-GECKO version for the July-August 2013 period. The simulated mean OA concentrations range from ~0 μg.m⁻³ in remote oceanic areas, to ~12 μg m⁻³ around the Adriatic Sea and in the northern Italy, and are coherent with the expected orders of magnitude and spatial distributions over Europe (Aksoyoglu et al., 2011; Crippa et al, 2014). Figure 2.b presents the relative difference between mean OA mass concentrations simulated with ref-VBS-GECKO and with H²O. The ref-VBS-GECKO produces more OA than H²O, with a mean OA mass concentration around 30% higher on average over Europe. The increase is particularly important over northern Europe, with maximum differences reaching around +60%.

8

Table 3 gathers the statistical results calculated on daily averaged concentrations for ref-VBS-GECKO at the 48 stations (RMSE, Pearson's r, MFB and MFE), as well as the difference of this statistical indicator between ref-VBS-GECKO and H^2O. Statistical indicators show a high spatiotemporal correlation between ref-VBS-GECKO and measurements for daily OM_{PM1} and $OC_{PM2.5}$ with $r > 0.5$ (0.79 and 0.57 respectively). These r values are in the standard of what has been found in

5   previous modeling studies for Europe (Bergström et al., 2012; Ciarelli et al., 2017) or USA (Ahmadov et al., 2012; Murphy et al., 2017). For daily averaged measurements of $PM_{2.5}$, the correlation is smaller (0.42). This lower correlation for $PM_{2.5}$ has already been highlighted in summertime during the EURODELTA-III inter-comparison campaign (Bessagnet et al., 2016). MFE and MFB satisfy the performance criteria of Boylan and Russel (2006) for all the measurements. However, daily averaged $PM_{2.5}$, and especially the organic fraction (OM_{PM1} and $OC_{PM2.5}$), appear to be systematically underestimated

10   by the ref-VBS-GECKO model.

Comparing ref-VBS-GECKO statistical results with H^2O statistical results, the simulated daily averaged $PM_{2.5}$ concentrations over the 36 stations appear to be weakly sensitive to the SOA formation mechanism used in the model. Only a slight improvement due to an increase in simulated $PM_{2.5}$ concentrations of about 5.5% is observed with the ref-VBS-GECKO model configuration. Concerning simulated $OC_{PM2.5}$ over the 13 measurement stations, the ref-VBS-GECKO

15   parameterization leads to an increase of the simulated concentration (+ 15.6 %), ultimately leading to a clear improvement of MFE, MFB and correlation. Nevertheless, using the ref-VBS-GECKO configuration instead of the H^2O configuration increases RMSE (+5%), owing to a substantial overestimation of OA. The main differences between the two organic aerosol modules are reached for OM_{PM1} with simulated ref-VBS-GECKO concentrations higher than H^2O by 31.5%. As simulated OM_{PM1} concentrations were highly underestimated using the former H^2O configuration compared to observations (6

20   stations), the ref-VBS-GECKO configuration improves RMSE, MFB and MFE.

Figure 3 shows comparisons between the measured and the simulated daily averaged temporal evolutions of OM_{PM1}, $OC_{PM2.5}$ and/or $PM_{2.5}$ concentrations at the 7 selected stations. Figure 4 shows the measured and simulated mean diurnal profiles at the 4 stations providing OM_{PM1}. Simulations capture qualitatively the observed feature of the daily averaged time series for $PM_{2.5}$, $OC_{PM2.5}$ and OM_{PM1}, and the mean diurnal profiles for OM_{PM1}. At stations dominantly impacted by biogenic sources,

25   OA concentrations simulated with ref-VBS-GECKO are higher than those simulated with H^2O, leading to a better agreement with measurements (see Fig. 3.d to h and Fig. 4.c and d). However, day/night variations of OM_{PM1} seem to be overestimated. At stations influenced by anthropogenic air masses, OA concentrations are weakly influenced by the organic aerosol module (see Fig. 3.a to c and Fig. 4.a and b). OA concentrations simulated with ref-VBS-GECKO are substantially underestimated, differences exceeding -50% for OM_{PM1} concentrations at the Palaiseau and Melpitz stations as well as for $OC_{PM2.5}$

30   concentrations at the Cabauw station.

4. Sensitivity to the parameterization properties

Sensitivity tests were performed to assess the VBS-GECKO parameterization, evaluate the consistency of the modeling results and examine some hypotheses that may explain the gaps between measurement and simulated values. Sensitivities to hydro-solubility, gaseous aging, NO_x regimes and volatility were studied comparing results to the non-modified ref-VBS-GECKO version.

4.1. Sensitivity tests to hydro-solubility and H^{eff}

SOA formation from the gas/particle partitioning of hydro-soluble organic compounds into an aqueous phase is now well recognized (e.g. Bregonzio-Rozier et al., 2016; Carlton et al., 2009; Knote et al., 2014). The effective Henry's law constant (H^{eff}) is the key parameter which controls this hydrophilic partitioning. Hydro-soluble organic compounds can also be lost at the surface by dry deposition. In CHIMERE, and according to the deposition scheme of Wesely (1989), the stomatal resistance of organic compounds depends on H^{eff}. To analyze the sensitivity of the simulated OA to hydrophilic partitioning and values of H^{eff}, the following two simulations were run:

- **Hydro-VBS-GECKO**. In this model configuration, $VB_{k,i}$ can condense both on organic and aqueous phases of particles. Aqueous-phase partitioning is computed according to Henry's law, assuming the particle phase behave as an ideal well mixed homogeneous aqueous phase. Deposition of $VB_{k,i}$ was already taken into account in the reference model configuration and was kept unchanged.

- **Hydro-VBS-GECKO-high**. This model configuration is identical to the hydro-VBS-GECKO configuration above, except that the original H^{eff} of each $VB_{k,i}$ are multiplied by 100. The new H^{eff} values correspond to the upper values of the H^{eff} distribution of secondary organic compounds contributing to a given volatility bin (see Lannuque et al., 2018).

The relative difference on the simulated mean OA concentrations between Hydro-VBS-GECKO (respectively Hydro-VBS-GECKO-high) and ref-VBS-GECKO is given Fig. 5.a (respectively Fig. 5.b) for the two-month period. Figure 5.a shows that considering aqueous phase partitioning of the VBS-GECKO species leads to variations on the simulated mean OA concentrations below ±0.5%. Table 4 shows no significant modification in the statistical results for this simulation. The values of H^{eff} set to each volatility bin increase when the volatility decreases (see Table 1), meaning that the less volatile species are also more prone to condense into the aqueous phase. Adding a hydrophilic partitioning does therefore not increase substantially the concentrations of organic species in the condensed phases.

The Hydro-VBS-GECKO-high configuration increases the mean simulated OA concentrations by ~10%, with a maximal increase reached over Belgium-Netherlands-Luxembourg area (called Benelux hereafter, around +20%, see Fig. 5.b). The contribution of the deposition and the partitioning processes are shown in Fig. 5.c and 5.d respectively. Changes due to deposition appear negligible (below ±0.2%) compared to the changes due to the aqueous partitioning (~+10%). According to the Wesely (1989) parameterization used for deposition, water solubility contributes to the surface resistance only. Knote et

10

al. (2014) have shown that deposition is not limited by the surface resistance for H^{eff} greater than 10^8 mol L^{-1} atm^{-1}. In the ref-VBS-GECKO, this threshold corresponds to the $VB_{k,(3-7)}$ nominal H_{eff} values, i.e. to the volatility bins partitioning mainly to OA. OA concentrations are therefore not sensitive to an increase of the H_{eff} values. The increase of H^{eff} by a factor of 100 makes possible hydrophilic partitioning of the most volatile bins that would not have condensed otherwise and leads to an increase of simulated OA concentrations. The maximum relative changes simulated over Benelux are mainly linked to the high relative humidity encountered in this area and the low simulated OA concentrations (see Fig. 2.a). This model configuration improves slightly the RMSE, MFB and MFE calculated on OM_{PM1} (-4.58 %, -0.06 and -0.05 respectively) and $OC_{PM2.5}$ (-0.65 %, -0.05 and -0.03 respectively) mass concentrations (see Table 4). According to these tests, SOA production due to the hydrophilic partitioning of the various $VB_{k,i}$ of the VBS-GECKO parameterization is expected to be a minor process.

4.2. Sensitivity test to gaseous aging rates and OH radical concentrations

In the VBS-GECKO parameterization, the same rate constant is set for the $VB_{k,i}$ reactions with OH (k_{OH} = 4.0×10^{-11} cm^3 molec^{-1} s^{-1}). Timescale for gaseous aging is therefore driven by the OH concentrations simulated by the CTM. Simulated OH concentrations depend on the gas-phase chemical mechanisms used in the CTM, with differences on OH concentrations reaching up to 45% between mechanisms (Sarwar et al., 2013). Two simulations were run with modified k_{OH} to examine the sensitivity of SOA production to the rate of chemical aging:

- **k_{OH}-VBS-GECKO-low**. In this model configuration, the $VB_{k,i}$+OH rate constants are divided by a factor 2, i.e. k_{OH}^{low} = 2.0×10^{-11} cm^3 molec^{-1} s^{-1}.
- **k_{OH}-VBS-GECKO-high**. In this model configuration, the $VB_{k,i}$+OH rate constants are multiplied by a factor 2, i.e. k_{OH}^{high} = 8.0×10^{-11} cm^3 molec^{-1} s^{-1}.

The relative difference on the simulated mean OA concentrations between k_{OH}-VBS-GECKO-low (respectively k_{OH}-VBS-GECKO-high) and ref-VBS-GECKO is given Fig. 6.a (respectively Fig. 6.b). A slight variation of simulated OA concentrations is found (lower than ±10%), with simulated OA concentrations decreasing with the decrease of aging rates and *vice versa*. This result highlights that the gas-phase aging of volatility bins in the VBS-GECKO parameterization promotes functionalization (formation of less volatile bins) rather than fragmentation (formation of more volatile bins), as already shown with tests conducted in box model (Lannuque et al., 2018). The highest relative differences are located over the Mediterranean Sea and North Africa, i.e. areas showing high OH and low OA concentrations (below 4 µg m^{-3}, see Fig. 2.a). The k_{OH}-VBS-GECKO-high configuration improves statistics, due to an overall increase of the simulated OA concentrations (and contrariwise for the k_{OH}-VBS-GECKO-low configuration) (see Table 4). However, the sensitivity of SOA to the gas-phase aging of the VBS-GECKO volatility bins remains weak and aging rates is likely not a major source of uncertainty.

4.3. Sensitivity test to the NO$_x$ regime

Similar to the OH discussion above, simulated HO$_2$ and NO concentrations in CTMs are linked to the gas-phase chemical mechanism used. The concentrations of these two species determine the value of the RRR ratio and therefore drive the aging of the various VB$_{k,i}$ (Lannuque et al., 2018). A sensitivity test was performed to examine the sensitivity of the simulated OA

5   to the chemical regime. HO$_2$ or NO concentrations can hardly be modified without changing all the simulation conditions. Here, two simulations were run modifying the k$_{RO2+HO2}$ value used to calculate the RRR:

- **RRR-VBS-GECKO-low**. In this model configuration, RRR ratio is calculated with k$_{RO2+HO2}$ multiplied by 2, i.e. k$_{RO2+HO2}^{RRRlow}$ = 4.4×10^{-11} cm^3 molec^{-1} s^{-1}.

- **RRR-VBS-GECKO-high**. In this model configuration, RRR ratio is calculated with k$_{RO2+HO2}$ divided by 2, i.e.
10   k$_{RO2+HO2}^{RRRhigh}$ = 1.1×10^{-11} cm^3 molec^{-1} s^{-1}.

Figure 7 presents the mean RRR ratio during the two-month period for both RRR-VBS-GECKO-low (Fig. 7.a) and RRR-VBS-GECKO-high model configurations (Fig. 7.b). The entire range of RRR ratio (from remote NO$_x$ conditions to high NO$_x$ conditions) is covered over Europe with the both model configuration. As expected, the urban, industrial and intense shipping transport areas such as Paris, the Channel, Benelux, northern Italy or Moscow are systematically in the high NO$_x$

15   regime (RRR close to 1) whereas remote areas over the seas (away from shipping tracks) are systematically in the remote NO$_x$ regime (RRR close to 0). Between these two extremes, the RRR ratio depends on the environmental and meteorological conditions at the location and, in this sensitivity study, on the model configuration for the RRR calculation. Current parameterizations for SOA formation only consider two extreme regimes corresponding to a high-NO$_x$ and a low-NO$_x$ condition. Criteria used to define high and low NO$_x$ differ from a study to another one but the parameterizations are usually

20   optimized at NO$_x$ values typical of rural conditions for low NO$_x$ (corresponding to a RRR ratio of ~0.6) and typical of urban conditions for high NO$_x$ (corresponding to a RRR ratio of ~1) (e.g. Hodzic et al., 2014; Lane et al., 2008). The range of RRR between 0.0 and 0.6 is therefore not considered in most of the parameterizations, although substantial changes in SOA formation were found within this range of RRR (Lannuque et al., 2018).

The relative difference on the simulated mean OA concentrations between RRR-VBS-GECKO-low (respectively RRR-VBS-
25   GECKO-high) and ref-VBS-GECKO is given Fig. 8.a (respectively Fig. 8.b). Results show variations of simulated mean OA concentrations smaller than ~15%. In agreement with previous studies, an increase (decrease) of RRR ratio leads to a decrease (increase) of the simulated OA concentrations (e.g. Donahue et al., 2005; Lannuque et al., 2018; Ng et al., 2007). As expected, the variation is weaker over areas having either an RRR ratio close to 0 or 1, the NO$_x$ regime remaining unchanged among the model configurations. The highest relative differences on OA are found over continental rural areas,

30   i.e. areas showing the largest variation of RRR among the model configurations. Large relative differences are also found over the Mediterranean Sea, owing in part to the low simulated OA concentrations. Similar to the k$_{OH}$ sensitivity tests, the RRR-VBS-GECKO-low configuration increases the overall OA concentrations and improves statistical indicators, and

contrariwise for the RRR-VBS-GECKO-high configuration. Sensitivity on RRR values appears weak enough to likely not be a major source of uncertainty for the VBS-GECKO parameterization.

4.4. Sensitivity test to volatility and P^{sat}

In the explicit GECKO-A simulations used for the VBS-GECKO optimization, the saturation vapor pressure, P^{sat}, of secondary organic compounds was estimated using structure activity relationships (SAR) (see Lannuque et al., 2018). Estimated P^{sat} can typically vary within one order of magnitude according to the SAR used (e.g. Valorso et al., 2011). Two simulations were run to examine the sensitivity of SOA to the uncertainties in P^{sat}:

- **P^{sat}-VBS-GECKO-low.** In this model configuration, the nominal P^{sat} values of $VB_{k,i}$ are divided by 10.
- **P^{sat}-VBS-GECKO-high.** In this model configuration, the nominal P^{sat} values of $VB_{k,i}$ are multiplied by 10.

As OA concentration directly contributes to the partitioning, these two simulations can also be considered as a sensitivity test to the simulated OA concentrations.

The relative difference on the simulated mean OA concentrations between P^{sat}-VBS-GECKO-low (respectively P^{sat}-VBS-GECKO-high) and ref-VBS-GECKO is given Fig. 9.a (respectively Fig. 9.b). Shifting the volatility of the $VB_{k,i}$ by one order of magnitude leads to an overall change in the simulated mean OA concentrations of about -25% (+25%) when P^{sat} is increased (decreased). A weaker sensitivity is observed over urban areas, such as Paris or Moscow. This behavior is mainly linked to the simulated volatility of OA in the ref-VBS-GECKO simulations. Figure 10 shows the mean volatility of OA over Europe for the reference configuration. Simulated OA contributors are mainly low volatile species (with mean P^{sat}_{298K} between 10^{-10} and 10^{-14} atm), the highest values being found over urban areas (less aged OA), and the lowest values found over areas close to the boundaries of the domain (linked to a boundary effect in the model). A shift in volatilities over these two types of site has a lower impact on OA concentrations, as OA mean volatilities being either too high (mean $P^{sat}_{298K} \approx 10^{-10}$ atm, upon urban areas) or too low (mean $P^{sat}_{298K} \approx 10^{-14}$ atm, upon boundary areas) for a change in P^{sat} to substantially impact the partitioning. The largest effect is typically observed over central Europe where OA contributors show intermediate mean volatilities (mean $P^{sat}_{298K} \approx 10^{-12}$ atm).

Statistically, the P^{sat}-VBS-GECKO-low configuration is the only configuration matching the performance goal for all the simulated OA concentrations ($OC_{PM2.5}$ and OM_{PM1}) (see Table 4). For $OC_{PM2.5}$, RMSE is however higher than in reference configuration. Simulated OA concentrations appear to be sensitive to uncertainties in the estimated saturation vapor pressures of the numerous OA contributors considered during the development of the VBS-GECKO parameterization.

5. Sensitivity to IVOC emission fluxes from traffic and transport sources

IVOCs have been shown to be a substantial source of SOA in the plume of megacities (e.g. Hodzic et al., 2010; Tsimpidi et al., 2010). Even if several recent studies have been performed to identify the IVOC speciation of different individual

13

emission sources (e.g. Akherati et al., 2019; Grieshop et al., 2009; Hatch et al., 2018; Jathar et al., 2017; Louvaris et al., 2017; Lu et al., 2018; May et al., 2013a, 2013b, 2013c; Woody et al., 2016), a comprehensive inventory is still not available to represent IVOC emissions by activity sector (gathering several individual emission sources). A large fraction of these IVOCs is thus still not considered in emission inventories. In this section, only IVOC emissions from traffic and transportation sources are treated. Robinson et al. (2007) assumed that IVOC emissions for small off-road diesel engines were equal to 150% of POA emissions, consistent with the Schauer et al. (1999) emission data for 1995 medium-duty diesel vehicles. Recent studies have measured IVOC emissions from (i) exhausts of light-duty gasoline vehicles and (ii) exhausts of both heavy-duty and medium-duty diesel vehicles (Zhao et al., 2015, 2016). Experiments on gasoline exhausts were processed on 42 vehicles and experiments on diesel vehicles on 6 vehicles, the selected vehicles being representative of the transportation fleet in North America. In both cases, Zhao et al. (2015, 2016) have shown that a stronger correlation can be found between IVOC and NMVOC emissions (R^2 equal to 0.92 and 0.98 for gasoline and diesel exhausts, respectively) than between IVOC and POA emissions (R^2 equal to 0.76 and 0.61 for gasoline and diesel exhausts, respectively). Zhao et al. (2015, 2016) have estimated that IVOC emissions represent about 4% of NMVOC emissions in cold-start cycle to about 16% in hot-start cycle for light-duty gasoline vehicles, and about 60 ± 10 % of NMVOC emissions for heavy-duty and medium-duty diesel vehicles.

In this study, the VBS-GECKO parameterization was used to examine the sensitivity of SOA to IVOC emissions from road traffic (SNAP 7) and other mobile sources and machineries (SNAP 8). The following five model configurations, based on different IVOC emission fluxes, were designed for that purpose:

- **IVOC$_{150POA}$**. In this model configuration, IVOC emissions are set to 150% of the semi-volatile POA emissions, based on Robinson et al. (2007).

- **IVOC$_{4VOC}$**. In this configuration, IVOC emissions are set to 4% of NMVOC emissions, based on Zhao et al. (2016) for gasoline vehicles in cold-start cycle.

- **IVOC$_{16VOC}$**. In this configuration, IVOC emissions are set to 16% of NMVOC emissions, based on Zhao et al. (2016) for gasoline vehicles in hot-start cycle.

- **IVOC$_{30VOC}$**. In this configuration, emissions are set to 30% of NMVOC emissions, assuming a mixing of diesel and gasoline vehicle fleets.

- **IVOC$_{65VOC}$**. In this configuration, IVOC emissions are set to 65% of NMVOC emissions, based on Zhao et al. (2015) for diesel vehicles.

As in the reference model configuration, POA are considered as SVOC in these sensitivity tests for traffic and transport emissions. Primary SVOCs and IVOCs (S/IVOCs) constitute a complex mixture of linear, branched and cyclic alkanes, alkenes and aromatics (Fraser et al., 1997; Gentner et al., 2012; Lu et al., 2018; Schauer et al., 1999, 2002). The molecular composition of S/IVOCs emitted in the atmosphere by fossil fuel combustion is however still poorly documented. S/IVOCs at emission were thus considered to be distributed into the 9 volatility bins given by Robinson et al. (2007), with the

14

provided fraction of primary SVOCs in each SVOC volatility bin, and of estimated primary IVOCs in each IVOC volatility bin. The VBS-GECKO parameterizations for C_{14}, C_{18}, C_{22} and C_{26} 1-alkenes and n-alkanes were used as surrogate mechanisms for S/IVOCs (C_{14} and C_{18} for IVOCs and C_{18}, C_{22} and C_{26} for SVOCs). The C_{14} to C_{26} VBS-GECKO's n-alkanes and 1-alkenes were distributed according to their volatility into the 9 volatility bins of Robinson et al. (2007).

5   Correspondences are shown in Figure 11, for the example of the $IVOC_{150POA}$ model configuration. The distribution of alkanes and alkenes was estimated based on (i) the EMEP guidebook (https://www.eea.europa.eu/publications/emep-eea-guidebook-2016), providing speciation data for emissions for various types of vehicles and (ii) the COPERT4 software (Ntziachristos et al., 2009) providing data for a vehicle fleet. Data are only available for light compounds and are here extrapolated to the heavy ones for the needs of the study. Thus, 75 % of the primary S/IVOCs are here assumed to be alkanes

10   and 25 % alkenes. The primary SVOC total emissions and distributions over volatility bins are unchanged between each simulation. The distribution of IVOCs among volatility bins is also unchanged but the total IVOC emissions are modulated according to the 5 IVOC emission scenarios described before (i.e. $IVOC_{150POA}$, $IVOC_{4VOC}$, $IVOC_{16VOC}$, $IVOC_{30VOC}$ and $IVOC_{65VOC}$). Table 5 gives the speciation of VBS-GECKO species for the various model configurations and the VBS-GECKO mechanism for S/IVOCs is presented in Table S3 of supplementary material.

15   Figure 12 shows the mean OA mass concentrations simulated for the 5 IVOC emission configurations, and the absolute and relative differences with the ref-VBS-GECKO simulation without IVOC emissions. Table 6 presents the statistical results calculated on daily averaged concentrations (RMSE, Pearson's correlation coefficient, MFE and MFB) for the different IVOC emission configurations, and their difference with those of the ref-VBS-GECKO configuration. As discussed previously, the highest concentrations are simulated over northern Italy (see Fig. 2). For this area, accounting for IVOC

20   emissions increases the simulated concentrations of OA up to 3 µg m^{-3} with the $IVOC_{65VOC}$ model configuration. As expected, OA concentration increases when IVOC emissions over Europe are taken into account during the simulated period, with an overall mean increase of about 12, 2, 5, 10 and 20% for the $IVOC_{150POA}$, $IVOC_{4VOC}$, $IVOC_{16VOC}$, $IVOC_{30VOC}$ and $IVOC_{65VOC}$ configuration, respectively. The relative differences show large increases of OA concentrations (reaching +40%) over a wide area including North Sea and Benelux for the $IVOC_{65VOC}$ configuration, owing to the low simulated OA

25   concentrations with the ref-VBS-GECKO configuration. The $IVOC_{150POA}$ configuration leads to mean OA mass concentrations lying between the $IVOC_{16VOC}$ and the $IVOC_{30VOC}$ configurations. Area showing substantial changes in simulated OA are however different between these model configurations. In the $IVOC_{150POA}$ configuration, the largest OA concentration increase is simulated over the Channel and Gibraltar's Detroit (up to +80%). These results were expected for this model configuration based on POA emissions. Indeed, ships are one of the most important sources of POA but emit a

30   relatively small amount of NMVOCs. For example, the EMEP inventory for 2013 estimates an average NMVOC/POA emission ratio of ~4 for road traffic in Europe and ~0.4 for shipping in the studied domain.

Taking into account SOA formation from IVOC precursors improves the statistical indicators for the simulated concentrations of OM_{PM1}. As discussed previously, the ref-VBS-GECKO configuration underestimates OM_{PM1}. Including IVOC emission increases the mean OM_{PM1} concentrations at the stations of about 5, 2, 5, 7 or 13% for the $IVOC_{150POA}$,

15

IVOC$_{4VOC}$, IVOC$_{16VOC}$, IVOC$_{30VOC}$ or IVOC$_{65VOC}$ configuration, respectively. Increasing IVOC emissions provide better statistical indicators for OM$_{PM1}$, with MFE and MFB significantly closer to the performance goal (MFE decreases by 0.06 and |MFB| decreases by 0.09 between IVOC$_{4VOC}$ and IVOC$_{65VOC}$ configurations, see Table 6). For OC$_{PM2.5}$ however, the opposite trend is observed with a degradation of the statistical indicators (Table 6). The ref-VBS-GECKO configuration

5 leads to a slight overestimation of OC$_{PM2.5}$ concentrations over some stations (e.g. Iskrba, see Fig. 3) and adding the SOA source from IVOCs strengthens the deviation (up to about +30% of RMSE for the IVOC$_{65VOC}$ configuration), even if the correlation is not significantly modified.

IVOC oxidation appears to be a significant SOA source at some locations (e.g. the Cabauw station), especially in the IVOC$_{30VOC}$ and IVOC$_{65VOC}$ configuration. However, the resulting OA increase remains too weak to fill in the gaps between

10 observations and simulated data (maximum increase around +40%). For example, time series presented in Figure 13 show that adding IVOC emission increases systematically the simulated OA concentrations, but not enough to explain the OA peaks recorded at the anthropogenic stations (see Fig. 13.b). Moreover, accounting for IVOC emission strengthens the disagreement of the simulated concentrations with observations over other areas (e.g. at Iskrba station).

The various IVOC emission configurations are aimed to answer to the question: with constant POA and NMVOC emissions

15 for the traffic, does IVOC emissions typical of diesel vehicles (upper limit) or gasoline vehicles (lower limit) significantly change OA concentrations in Europe, and in particular in anthropogenic areas? At a local scale where anthropogenic sources are dominant, IVOC emissions from traffic and transportation sources appear to be a significant source of OA and simulated OA concentrations are dependent to the IVOC emission configuration (~+3 µg m^{-3} in northern Italy for IVOC$_{65VOC}$ against IVOC$_{4VOC}$). At a continental scale outside anthropogenic areas, the low variations observed on simulated OA concentrations

20 between the different IVOC emission configurations suggest that IVOCs from traffic and transportation sources are likely not a major source of SOA.

6. Tracking OA sources

Apportionment of OA sources is investigated in this section. The study takes into account OA formation from IVOC oxidation and is based on the IVOC$_{30VOC}$ model configuration. Figure 14 shows the contribution of the various OA sources

25 to the simulated OA concentrations during the July-August 2013 period and the mean daily profiles at two stations located in areas dominantly impacted by anthropogenic air masses (Cabauw and Palaiseau) and two stations located in areas dominantly impacted by biogenic air masses (Birkenes II and Iskrba). SOA constitutes the main fraction of OA whatever the environment. This secondary fraction typically grows from anthropogenic impacted areas (about 70 % at Palaiseau station) to remote areas (about 95 % at Iskrba station). This trend is in agreement with what is usually observed or simulated for

30 summertime periods (e.g. Aksoyoglu et al. 2011; Belis et al., 2013). For the remote stations Birkenes II and Iskrba, respectively 82 and 67% of the simulated OA concentration comes from a biogenic source. Contrariwise, anthropogenic

sources are the major OA contributors at anthropogenic impacted stations (65 and 60% of OA at the Cabauw and Palaiseau stations, respectively.

Among OA biogenic sources, terpene oxidation is clearly found as the major contributor of OA during the summer period, contributing from 35% (at anthropogenic impacted stations) to 80% (at remote stations) of the total OA mass. The 60%
5   increase of OA mass concentration observed in north Europe between H^2O and VBS-GECKO parameterizations (see Fig. 2) is also mainly related to SOA formation from terpene, especially ocimene and limonene. In our simulation, SOA produced by isoprene oxidation does not represent a substantial fraction of OA at the selected measurement stations. The major contribution of isoprene SOA to OA reaches about 5% (see Fig. 14.h) and is observed at the Iskrba station during diurnal conditions.

10   The anthropogenic fraction of OA is found to be dominated by residential biomass burning sources (BBOA). Indeed, according to the temporal factors used in CHIMERE (based on GENEMIS, Ebel et al., 1997; Friedrich, 2000), 4% of annual emissions of residential BBOA occurs during July-August, leading to a non-negligible amount of residential BBOA during summer. This result remains however subject to caution, owing to the large uncertainties in the temporalization of biomass burning emissions in the model. The primary organic fraction (i.e. condensed primary SVOCs) from traffic emissions is
15   found to be substantial in the OA budget only at night in urban areas. On the other hand, the secondary organic fraction produced by traffic emissions can represent about 50% of diurnal anthropogenic OA at stations near urban areas (i.e. Palaiseau and Cabauw). OA formed by the oxidation of mono-aromatic species is found to be negligible over Europe (less than 0.025 µg m^{-3} on average over the studied domain). Figure 15 shows the contribution of traffic emission to the simulated OA concentrations for the July-August 2013 period for 3 categories of precursors: SVOCs, IVOCs and mono-aromatic
20   compounds. As mentioned above, the OA concentrations from mono-aromatic compound oxidation are negligible compared to concentrations from traffic S/IVOC oxidation. Globally, in our study over Europe, OA concentrations produced from traffic S/IVOC oxidation are of the same order of magnitude. OA from primary SVOCs is locally more important close to sources (i.e. Northern Italy, Moscow, Paris, Gibraltar, etc). OA from IVOC is globally higher far away from the sources, with a higher dispersion over Europe (Fig. 15). This higher dispersion is expected owing to the larger timescale required to
25   produce low volatility species via multistep oxidation processes in the plumes of high emission area.

The distributions of OA within the volatility bins (given in Figure S2 of supplementary material) show similar features from one station to another. The results suggest that OA over Europe has relatively low volatility during summertime. Indeed, the VBS-GECKO contributors to OA have very low volatility: ~80% of the OA contributors from VBS-GECKO are volatility bins 7 to 5 ($VB_{k,7}$, $VB_{k,6}$ and $VB_{k,5}$ species), i.e. having saturation vapor pressure at 298 K of 10^{-14}, 10^{-12} and 10^{-11} atm
30   respectively.

7. Conclusions

The VBS-GECKO parameterization for SOA production was developed based on explicit mechanisms generated with the GECKO-A tool. The VBS-GECKO parameterization was fitted using box modelling results for a selected set of parent compounds including terpenes, mono-aromatic compounds, linear alkanes and alkenes and for various environmental conditions, including different NO_x regimes, temperatures, OA loads (Lannuque et al., 2018). In this study, the VBS-GECKO parameterization was evaluated in the CHIMERE β 2017 CTM over Europe during summertime.

The VBS-GECKO parameterization shows good performances to simulate OA concentrations over Europe in the summer. Calculated mean fractional biases and mean fractional errors on $PM_{2.5}$, $OC_{PM2.5}$ and OM_{PM1} satisfy the performance criteria of Boylan and Russel (2006). The model configuration including the VBS-GECKO parameterization yields to higher OA concentrations compared to the former reference configuration including the H^2O parameterization. The deviations between the two configurations are especially marked over northern Europe, with an increase factor of ~60%. Outside this area, the OA increases obtained with the VBS-GECKO configuration are slight. Statistically, the use of the VBS-GECKO improves the overall MFB, MFE and RMSE and does not modify significantly correlation coefficients. Tests performed to examine the sensitivity of simulated OA concentrations to hydro-solubility, volatility, aging rates and NO_x regimes have shown that the VBS-GECKO parameterization provides consistent results that are not subject to large deviations induced by parameters provided by the gas phase mechanism included in the CTM (e.g. HO_x or NO_x concentrations). However, the OA concentrations remain underestimated with the VBS-GECKO model configuration, especially in areas with a significant contribution of anthropogenic sources (e.g. reaching a factor of 2.5 for $OC_{PM2.5}$ at the NL0644R station in Netherlands). None of the conducted sensitivity test leads to OA variations large enough to fill the gaps between measurements and simulated concentrations at the anthropogenic stations.

The analysis of simulated OA shows that, during summertime, the main fraction is made of secondary matter which represents ~85% of the total mean OA concentration. A large fraction of the simulated OA comes from biogenic sources (between 30 and 85% of the total OA), especially from terpene oxidation which represents ~95% of these biogenic sources. For the conditions examined in this study, OA formed by the oxidation of mono-aromatic compounds appears to be negligible with maximum mean concentrations of 0.025 μg m^{-3} over North Sea and Benelux. Note that ignoring SOA production from these precursors in the model would substantially reduce the number of $VB_{k,i}$ species currently considered in the VBS-GECKO parameterization. The simulated OA was found to be made of species having low and extremely low volatilities in remote areas, but also of SVOCs closer to major anthropogenic sources.

Finally, IVOC oxidation was added to examine the contribution of this additional source to the SOA budget. Five model configurations with distinct IVOC emissions from traffic were tested and compared using the VBS-GECKO parameterization in CHIMERE. As expected, considering the emission of IVOCs by traffic and transport sources was found to globally increase background OA concentrations. Although SOA production from traffic IVOC oxidation can locally be significant (up to ~+3 μg m^{-3} in northern Italy, assuming IVOC emissions represents 65% of NMVOC emissions), this

additional OA source remains too small to explain the gap between simulated and measured values at stations where anthropogenic sources are dominant. This first application of this new VBS-GECKO parameterization has been shown to provide consistent results. This outcome creates motivation to extend the exploration to wintertime conditions, and expand the list of parent compounds considered, in particular to include SOA formation from oxidation of isoprene, sesquiterpenes

5   or organics species emitted by residential biomass burning, a prerequisite to extend the evaluation and analysis to wintertime when this source is dominant. This is the subject of ongoing studies. The VBS-GECKO is a heavy parameterization in term of species number. Calculation time is multiplied by two using the complete VBS-GECKO scheme with IVOCs compared to H^2O. This study has shown that the number of species can be optimized. For example, because of the low influence on OA concentrations, the representation of the SOA formed by the oxidation of mono-aromatic species can be highly simplified

10 and C_{10} precursors even removed.

Author Contribution

VL implemented the parameterization in the air quality model and conducted the simulations and the sensitivity tests. All the authors contributed to design the research, to interpret the data and to write the article.

References

Akherati, A., Cappa, C. D., Kleeman, M. J., Docherty, K. S., Jimenez, J. L., Griffith, S. M., Dusanter, S., Stevens, P. S. and Jathar, S. H.: Simulating secondary organic aerosol in a regional air quality model using the statistical oxidation model - Part 3: Assessing the influence of semi-volatile and intermediate-volatility organic compounds and NOx, Atmos. Chem. Phys.,

5   19(7), 4561–4594, https://doi.org/10.5194/acp-19-4561-2019, 2019.

Aksoyoglu, S., Keller, J., Barmpadimos, I., Oderbolz, D., Lanz, V. A., Prévât, A. S. H. and Baltensperger, U.: Aerosol modelling in Europe with a focus on Switzerland during summer and winter episodes, Atmos. Chem. Phys., 11(14), 7355–7373, https://doi.org/10.5194/acp-11-7355-2011, 2011.

Aumont, B., Szopa, S. and Madronich, S.: Modelling the evolution of organic carbon during its gas-phase tropospheric

10   oxidation: development of an explicit model based on a self generating approach, Atmos. Chem. Phys., 5(9), 2497–2517, https://doi.org/10.5194/acp-5-2497-2005, 2005.

Belis, C. A., Karagulian, F., Larsen, B. R. and Hopke, P. K.: Critical review and meta-analysis of ambient particulate matter source apportionment using receptor models in Europe, Atmos. Environ., 69, 94–108, https://doi.org/10.1016/j.atmosenv.2012.11.009, 2013.

15   Bergström, R., Denier Van Der Gon, H. A. C., Prévôt, A. S. H., Yttri, K. E. and Simpson, D.: Modelling of organic aerosols over Europe (2002-2007) using a volatility basis set (VBS) framework: Application of different assumptions regarding the formation of secondary organic aerosol, Atmos. Chem. Phys., 12(18), 8499–8527, https://doi.org/10.5194/acp-12-8499-2012, 2012.

Bessagnet, B., Hodzic, A., Vautard, R., Beekmann, M., Cheinet, S., Honoré, C., Liousse, C. and Rouil, L.: Aerosol modeling

20   with CHIMERE - Preliminary evaluation at the continental scale, Atmos. Environ., 38(18), 2803–2817, https://doi.org/10.1016/j.atmosenv.2004.02.034, 2004.

Bessagnet, B., Menut, L., Curci, G., Hodzic, A., Guillaume, B., Liousse, C., Moukhtar, S., Pun, B., Seigneur, C. and Schulz, M.: Regional modeling of carbonaceous aerosols over Europe—focus on secondary organic aerosols, J. Atmos. Chem., 61(3), 175–202, https://doi.org/10.1007/s10874-009-9129-2, 2009.

25   Bessagnet, B., Seigneur, C. and Menut, L.: Impact of dry deposition of semi-volatile organic compounds on secondary organic aerosols, Atmos. Environ., 44(14), 1781–1787, https://doi.org/10.1016/j.atmosenv.2010.01.027, 2010.

Bessagnet, B., Pirovano, G., Mircea, M., Cuvelier, C., Aulinger, A., Calori, G., Ciarelli, G., Manders, A., Stern, R., Tsyro, S., Garciá Vivanco, M., Thunis, P., Pay, M. T., Colette, A., Couvidat, F., Meleux, F., Rouïl, L., Ung, A., Aksoyoglu, S., Baldasano, J. M., Bieser, J., Briganti, G., Cappelletti, A., D'Isidoro, M., Finardi, S., Kranenburg, R., Silibello, C., Carnevale,

30   C., Aas, W., Dupont, J. C., Fagerli, H., Gonzalez, L., Menut, L., Prévôt, A. S. H., Roberts, P. and White, L.: Presentation of the EURODELTA III intercomparison exercise-evaluation of the chemistry transport models' performance on criteria pollutants and joint analysis with meteorology, Atmos. Chem. Phys., 16(19), 12667–12701, https://doi.org/10.5194/acp-16-12667-2016, 2016.

Boucher, O., Randall, D., Artaxo, P., Bretherton, C., Feingold, G., Forster, P., Kerminen, V.-M., Kondo, Y., Liao, H., Lohmann, U., Rasch, P., Satheesh, S. K., Sherwood, S., Stevens, B. and Zhang, X. Y.: Clouds and Aerosols, in Climate Change 2013 - The Physical Science Basis. Contribution of Working Group I to the Fifth Assessment Report of the Intergovernmental Panel on Climate Change, edited by T. F. Stocker, D. Qin, G.-K. Plattner, M. Tignor, S. K. Allen, J.

5   Boschung, A. Nauels, Y. Xia, V. Bex, and P. M. Midgley, pp. 571–658, Cambridge University Press, Cambridge, United Kingdom and New York, NY, USA., 2013.

Boylan, J. W. and Russell, A. G.: PM and light extinction model performance metrics, goals, and criteria for three-dimensional air quality models, Atmos. Environ., 40(26), 4946–4959, https://doi.org/10.1016/j.atmosenv.2005.09.087, 2006.

Bregonzio-Rozier, L., Giorio, C., Siekmann, F., Pangui, E., Morales, S. B., Temime-Roussel, B., Gratien, A., Michoud, V.,

10   Cazaunau, M., Dewitt, H. L., Tapparo, A., Monod, A. and Doussin, J. F.: Secondary organic aerosol formation from isoprene photooxidation during cloud condensation-evaporation cycles, Atmos. Chem. Phys., 16(3), 1747–1760, https://doi.org/10.5194/acp-16-1747-2016, 2016.

Camredon, M., Aumont, B., Lee-Taylor, J. and Madronich, S.: The SOA/VOC/NOx system: an explicit model of secondary organic aerosol formation, Atmos. Chem. Phys., 7(21), 5599–5610, https://doi.org/10.5194/acp-7-5599-2007, 2007.

15   Canagaratna, M. R., Jimenez, J. L., Kroll, J. H., Chen, Q., Kessler, S. H., Massoli, P., Hildebrandt Ruiz, L., Fortner, E., Williams, L. R., Wilson, K. R., Surratt, J. D., Donahue, N. M., Jayne, J. T. and Worsnop, D. R.: Elemental ratio measurements of organic compounds using aerosol mass spectrometry: Characterization, improved calibration, and implications, Atmos. Chem. Phys., 15(1), 253–272, https://doi.org/10.5194/acp-15-253-2015, 2015.

Cappa, C. D. and Wilson, K. R.: Multi-generation gas-phase oxidation, equilibrium partitioning, and the formation and

20   evolution of secondary organic aerosol, Atmos. Chem. Phys., 12, 9505–9528, https://doi.org/10.5194/acp-12-9505-2012, 2012.

Cappa, C. D., Jathar, S. H., Kleeman, M. J., Docherty, K. S., Jimenez, J. L., Seinfeld, J. H. and Wexler, A. S.: Simulating secondary organic aerosol in a regional air quality model using the statistical oxidation model - Part 2: Assessing the influence of vapor wall losses, Atmos. Chem. Phys., 16(5), 3041–3059, https://doi.org/10.5194/acp-16-3041-2016, 2016.

25   Carlton, A. G., Wiedinmyer, C. and Kroll, J. H.: A review of Secondary Organic Aerosol (SOA) formation from isoprene, Atmos. Chem. Phys., 9(14), 4987–5005, https://doi.org/10.5194/acp-9-4987-2009, 2009.

Carter, W. P. L.: A detailed mechanism for the gas-phase atmospheric reactions of organic compounds, Atmos. Environ., 24(3), 481–518, https://doi.org/10.1016/0960-1686(90)90005-8, 1990.

Ciarelli, G., Aksoyoglu, S., El Haddad, I., Bruns, E. A., Crippa, M., Poulain, L., Äijälä, M., Carbone, S., Freney, E.,

30   O'Dowd, C., Baltensperger, U. and Prévôt, A. S. H.: Modelling winter organic aerosol at the European scale with CAMx: Evaluation and source apportionment with a VBS parameterization based on novel wood burning smog chamber experiments, Atmos. Chem. Phys., 17(12), 7653–7669, https://doi.org/10.5194/acp-17-7653-2017, 2017.

21

Ciarelli, G., Aksoyoglu, S., Crippa, M., Jimenez, J. L., Nemitz, E., Sellegri, K., Äijälä, M., Carbone, S., Mohr, C., O'dowd, C., Poulain, L., Baltensperger, U. and Prévôt, A. S. H.: Evaluation of European air quality modelled by CAMx including the volatility basis set scheme, Atmos. Chem. Phys., 16(16), 10313–10332, https://doi.org/10.5194/acp-16-10313-2016, 2016.

Couvidat, F. and Sartelet, K.: The Secondary Organic Aerosol Processor (SOAP v1.0) model: a unified model with different

5   ranges of complexity based on the molecular surrogate approach, Geosci. Model Dev., 8(4), 1111–1138, https://doi.org/10.5194/gmd-8-1111-2015, 2015.

Couvidat, F. and Seigneur, C.: Modeling secondary organic aerosol formation from isoprene oxidation under dry and humid conditions, Atmos. Chem. Phys., 11(2), 893–909, https://doi.org/10.5194/acp-11-893-2011, 2011.

Couvidat, F., Debry, É., Sartelet, K. and Seigneur, C.: A hydrophilic/hydrophobic organic (H2O) aerosol model:

10 Development, evaluation and sensitivity analysis, J. Geophys. Res., 117(D10), D10304, https://doi.org/10.1029/2011JD017214, 2012.

Couvidat, F., Kim, Y., Sartelet, K., Seigneur, C., Marchand, N. and Sciare, J.: Modeling secondary organic aerosol in an urban area: Application to Paris, France, Atmos. Chem. Phys., 13(2), 983–996, https://doi.org/10.5194/acp-13-983-2013, 2013.

15 Couvidat, F., Bessagnet, B., Garcia-Vivanco, M., Real, E., Menut, L. and Colette, A.: Development of an inorganic and organic aerosol model (CHIMERE 2017β v1.0): seasonal and spatial evaluation over Europe, Geosci. Model Dev., 11(1), 165–194, https://doi.org/10.5194/gmd-11-165-2018, 2018.

Crippa, M., Canonaco, F., Lanz, V. A., Äijälä, M., Allan, J. D., Carbone, S., Capes, G., Ceburnis, D., Dall'Osto, M., Day, D. A., DeCarlo, P. F., Ehn, M., Eriksson, A., Freney, E., Ruiz, L. H., Hillamo, R., Jimenez, J. L., Junninen, H., Kiendler-Scharr,

20 A., Kortelainen, A. M., Kulmala, M., Laaksonen, A., Mensah, A. A., Mohr, C., Nemitz, E., O'Dowd, C., Ovadnevaite, J., Pandis, S. N., Petäjä, T., Poulain, L., Saarikoski, S., Sellegri, K., Swietlicki, E., Tiitta, P., Worsnop, D. R., Baltensperger, U. and Prévôt, A. S. H.: Organic aerosol components derived from 25 AMS data sets across Europe using a consistent ME-2 based source apportionment approach, Atmos. Chem. Phys., 14(12), 6159–6176, https://doi.org/10.5194/acp-14-6159-2014, 2014.

25 Debry, E., Fahey, K., Sartelet, K., Sportisse, B. and Tombette, M.: Technical Note: A new SIze REsolved Aerosol Model (SIREAM), Atmos. Chem. Phys., 7(6), 1537–1547, https://doi.org/10.5194/acp-7-1537-2007, 2007.

Denier Van Der Gon, H. A. C., Bergström, R., Fountoukis, C., Johansson, C., Pandis, S. N., Simpson, D. and Visschedijk, A. J. H.: Particulate emissions from residential wood combustion in Europe - revised estimates and an evaluation, Atmos. Chem. Phys., 15(11), 6503–6519, https://doi.org/10.5194/acp-15-6503-2015, 2015.

30 Denkenberger, K. A., Moffet, R. C., Holecek, J. C., Rebotier, T. P. and Prather, K. A.: Real-time, single-particle measurements of oligomers in aged ambient aerosol particles, Environ. Sci. Technol., 41(15), 5439–5446, https://doi.org/10.1021/es070329l, 2007.

Dommen, J., Metzger, A., Duplissy, J., Kalberer, M., Alfarra, M. R., Gascho, A., Weingartner, E., Prevot, A. S. H., Verheggen, B. and Baltensperger, U.: Laboratory observation of oligomers in the aerosol from isoprene/NO x photooxidation, Geophys. Res. Lett., 33(13), 1–5, https://doi.org/10.1029/2006GL026523, 2006.

Donahue, N. M., Huff Hartz, K. E., Chuong, B., Presto, A. A., Stanier, C. O., Rosenhorn, T., Robinson, A. L. and Pandis, S. N.: Critical factors determining the variation in SOA yields from terpene ozonolysis: A combined experimental and computational study, Faraday Discuss., 130, 295–309, https://doi.org/10.1039/b417369d, 2005.

Donahue, N. M., Robinson, a. L., Stanier, C. O. and Pandis, S. N.: Coupled partitioning, dilution, and chemical aging of semivolatile organics, Environ. Sci. Technol., 40(8), 2635–2643, https://doi.org/10.1021/es052297c, 2006.

Donahue, N. M., Kroll, J. H., Pandis, S. N. and Robinson, A. L.: A two-dimensional volatility basis set – Part 2: Diagnostics of organic-aerosol evolution, Atmos. Chem. Phys., 12(2), 615–634, https://doi.org/10.5194/acp-12-615-2012, 2012.

Ebel, A., Friedrich, R. and Rodhe, H.: GENEMIS: Assessment, Improvement, and Temporal and Spatial Disaggregation of European Emission Data, in Tropospheric Modelling and Emission Estimation, pp. 181–214, Springer Berlin Heidelberg, Berlin, Heidelberg., 1997.

Emmons, L. K., Walters, S., Hess, P. G., Lamarque, J.-F., Pfister, G. G., Fillmore, D., Granier, C., Guenther, A., Kinnison, D., Laepple, T., Orlando, J., Tie, X., Tyndall, G., Wiedinmyer, C., Baughcum, S. L. and Kloster, S.: Description and evaluation of the Model for Ozone and Related chemical Tracers, version 4 (MOZART-4), Geosci. Model Dev., 3(1), 43–67, https://doi.org/10.5194/gmd-3-43-2010, 2010.

Fountoukis, C. and Nenes, A.: ISORROPIA II: a computationally efficient thermodynamic equilibrium model for K+–Ca2+–Mg2+–NH4+–Na+–SO42−–NO3, Atmos. Chem. Phys., 7(17), 4639–4659, https://doi.org/10.5194/acp-7-4639-2007, 2007.

Fraser, M., Cass, G., Simoneit, B. and Rasmussen, R.: Air quality model evaluation data for organics .4. C2-C36 non-aromatic hydrocarbons, Environ. Sci. Technol., 31(8), 2356–2367, https://doi.org/10.1021/es960980g, 1997.

Fredenslund, A., Jones, R. L. and Prausnitz, J. M.: Group-contribution estimation of activity coefficients in nonideal liquid mixtures, AIChE J., 21(6), 1086–1099, https://doi.org/10.1002/aic.690210607, 1975.

Friedrich, R.: GENEMIS: Generation of European Emission Data for Episodes, in Transport and Chemical Transformation of Pollutants in the Troposphere, pp. 375–386, Springer Berlin Heidelberg, Berlin, Heidelberg., 2000.

Gelencsér, A., May, B., Simpson, D., Sánchez-Ochoa, A., Kasper-Giebl, A., Puxbaum, H., Caseiro, A., Pio, C. and Legrand, M.: Source apportionment of PM2.5 organic aerosol over Europe: Primary/secondary, natural/anthropogenic, and fossil/biogenic origin, J. Geophys. Res., 112(D23), D23S04, https://doi.org/10.1029/2006JD008094, 2007.

Gentner, D. R., Isaacman, G., Worton, D. R., Chan, A. W. H., Dallmann, T. R., Davis, L., Liu, S., Day, D. A., Russell, L. M., Wilson, K. R., Weber, R., Guha, A., Harley, R. A. and Goldstein, A. H.: Elucidating secondary organic aerosol from diesel and gasoline vehicles through detailed characterization of organic carbon emissions, Proc. Natl. Acad. Sci., 109(45), 18318–18323, https://doi.org/10.1073/pnas.1212272109/-/DCSupplemental.www.pnas.org/cgi/doi/10.1073/pnas.1212272109, 2012.

de Gouw, J. A., Middlebrook, A. M., Warneke, C., Goldan, P. D., Kuster, W. C., Roberts, J. M., Fehsenfeld, F. C., Worsnop, D. R., Canagaratna, M. R., Pszenny, A. A. P., Keene, W. C., Marchewka, M., Bertman, S. B. and Bates, T. S.: Budget of organic carbon in a polluted atmosphere: Results from the New England Air Quality Study in 2002, J. Geophys. Res., 110(D16), D16305, https://doi.org/10.1029/2004JD005623, 2005.

5 Guenther, A. B., Jiang, X., Heald, C. L., Sakulyanontvittaya, T., Duhl, T., Emmons, L. K. and Wang, X.: The model of emissions of gases and aerosols from nature version 2.1 (MEGAN2.1): An extended and updated framework for modeling biogenic emissions, Geosci. Model Dev., 5(6), 1471–1492, https://doi.org/10.5194/gmd-5-1471-2012, 2012.

Han, S., Bian, H., Zhang, Y., Wu, J., Wang, Y., Tie, X., Li, Y., Li, X. and Yao, Q.: Effect of Aerosols on Visibility and Radiation in Spring 2009 in Tianjin, China, Aerosol Air Qual. Res., 12, 211–217, https://doi.org/10.4209/aaqr.2011.05.0073, 10 2012.

Hatch, L. E., Rivas-Ubach, A., Jen, C. N., Lipton, M., Goldstein, A. H. and Barsanti, K. C.: Measurements of I/SVOCs in biomass-burning smoke using solid-phase extraction disks and two-dimensional gas chromatography, Atmos. Chem. Phys., 18(24), 17801–17817, https://doi.org/10.5194/acp-18-17801-2018, 2018.

Heald, C. L., Jacob, D. J., Park, R. J., Russell, L. M., Huebert, B. J., Seinfeld, J. H., Liao, H. and Weber, R. J.: A large 15 organic aerosol source in the free troposphere missing from current models, Geophys. Res. Lett., 32(18), n/a-n/a, https://doi.org/10.1029/2005GL023831, 2005.

Hodzic, A., Jimenez, J. L., Madronich, S., Canagaratna, M. R., DeCarlo, P. F., Kleinman, L. and Fast, J.: Modeling organic aerosols in a megacity: potential contribution of semi-volatile and intermediate volatility primary organic compounds to secondary organic aerosol formation, Atmos. Chem. Phys., 10(12), 5491–5514, https://doi.org/10.5194/acp-10-5491-2010, 20 2010.

Hodzic, A., Aumont, B., Knote, C., Lee-Taylor, J., Madronich, S. and Tyndall, G.: Volatility dependence of Henry's law constants of condensable organics: Application to estimate depositional loss of secondary organic aerosols, Geophys. Res. Lett., 41(13), 4795–4804, https://doi.org/10.1002/2014GL060649, 2014.

Im, U., Bianconi, R., Solazzo, E., Kioutsioukis, I., Badia, A., Balzarini, A., Baró, R., Bellasio, R., Brunner, D., Chemel, C., 25 Curci, G., Flemming, J., Forkel, R., Giordano, L., Jiménez-Guerrero, P., Hirtl, M., Hodzic, A., Honzak, L., Jorba, O., Knote, C., Kuenen, J. J. P., Makar, P. A., Manders-Groot, A., Neal, L., Pérez, J. L., Pirovano, G., Pouliot, G., San Jose, R., Savage, N., Schroder, W., Sokhi, R. S., Syrakov, D., Torian, A., Tuccella, P., Werhahn, J., Wolke, R., Yahya, K., Zabkar, R., Zhang, Y., Zhang, J., Hogrefe, C. and Galmarini, S.: Evaluation of operational on-line-coupled regional air quality models over Europe and North America in the context of AQMEII phase 2. Part I: Ozone, Atmos. Environ., 115, 404–420, 30 https://doi.org/10.1016/j.atmosenv.2014.09.042, 2015.

Jacobson, M. Z., Turco, R. P., Jensen, E. J. and Toon, O. B.: Modeling coagulation among particles of different composition and size, Atmos. Environ., 28(7), 1327–1338, https://doi.org/10.1016/1352-2310(94)90280-1, 1994.

Jathar, S. H., Cappa, C. D., Wexler, a. S., Seinfeld, J. H. and Kleeman, M. J.: Multi-generational oxidation model to simulate secondary organic aerosol in a 3-D air quality model, Geosci. Model Dev., 8(8), 2553–2567, https://doi.org/10.5194/gmd-8-2553-2015, 2015.

5   Jathar, S. H., Woody, M., Pye, H. O. T., Baker, K. R. and Robinson, A. L.: Chemical transport model simulations of organic aerosol in southern California: Model evaluation and gasoline and diesel source contributions, Atmos. Chem. Phys., 17(6), 4305–4318, https://doi.org/10.5194/acp-17-4305-2017, 2017.

Jimenez, J. L., Canagaratna, M. R., Donahue, N. M., Prevot, A. S. H., Zhang, Q., Kroll, J. H., DeCarlo, P. F., Allan, J. D., Coe, H., Ng, N. L., Aiken, A. C., Docherty, K. S., Ulbrich, I. M., Grieshop, A. P., Robinson, A. L., Duplissy, J., Smith, J. D., Wilson, K. R., Lanz, V. A., Hueglin, C., Sun, Y. L., Tian, J., Laaksonen, A., Raatikainen, T., Rautiainen, J., Vaattovaara, P.,

10   Ehn, M., Kulmala, M., Tomlinson, J. M., Collins, D. R., Cubison, M. J., Dunlea, E. J., Huffman, J. A., Onasch, T. B., Alfarra, M. R., Williams, P. I., Bower, K., Kondo, Y., Schneider, J., Drewnick, F., Borrmann, S., Weimer, S., Demerjian, K., Salcedo, D., Cottrell, L., Griffin, R., Takami, A., Miyoshi, T., Hatakeyama, S., Shimono, A., Sun, J. Y., Zhang, Y. M., Dzepina, K., Kimmel, J. R., Sueper, D., Jayne, J. T., Herndon, S. C., Trimborn, A. M., Williams, L. R., Wood, E. C., Middlebrook, A. M., Kolb, C. E., Baltensperger, U. and Worsnop, D. R.: Evolution of organic aerosols in the atmosphere.,

15   Science (80-.)., 326(5959), 1525–9, https://doi.org/10.1126/science.1180353, 2009.

Johnson, D., Utembe, S. R., Jenkin, M. E., Derwent, R. G., Hayman, G. D., Alfarra, M. R., Coe, H. and McFiggins, G.: Simulating regional scale secondary organic aerosol formation during the TORCH 2003 campaign in the southern UK, Atmos. Chem. Phys., 6, 419–431, https://doi.org/10.5194/acpd-5-7829-2005, 2006.

Kalberer, M., Sax, M. and Samburova, V.: Molecular size evolution of oligomers in organic aerosols collected in urban

20   atmospheres and generated in a smog chamber, Environ. Sci. Technol., 40(19), 5917–5922, https://doi.org/10.1021/es0525760, 2006.

Knote, C., Hodzic, A., Jimenez, J. L., Volkamer, R., Orlando, J. J., Baidar, S., Brioude, J., Fast, J., Gentner, D. R., Goldstein, A. H., Hayes, P. L., Knighton, W. B., Oetjen, H., Setyan, A., Stark, H., Thalman, R., Tyndall, G., Washenfelder, R., Waxman, E. and Zhang, Q.: Simulation of semi-explicit mechanisms of SOA formation from glyoxal in aerosol in a 3-D

25   model, Atmos. Chem. Phys., 14(12), 6213–6239, https://doi.org/10.5194/acp-14-6213-2014, 2014.

Kroll, J. H. and Seinfeld, J. H.: Chemistry of secondary organic aerosol: Formation and evolution of low-volatility organics in the atmosphere, Atmos. Environ., 42(16), 3593–3624, https://doi.org/10.1016/j.atmosenv.2008.01.003, 2008.

Kulmala, M., Laaksonen, A. and Pirjola, L.: Parameterizations for sulfuric acid/water nucleation rates, J. Geophys. Res. Atmos., 103(D7), 8301–8307, https://doi.org/10.1029/97JD03718, 1998.

30   La, Y. S., Camredon, M., Ziemann, P. J., Valorso, R., Matsunaga, A., Lannuque, V., Lee-Taylor, J., Hodzic, A., Madronich, S. and Aumont, B.: Impact of chamber wall loss of gaseous organic compounds on secondary organic aerosol formation: Explicit modeling of SOA formation from alkane and alkene oxidation, Atmos. Chem. Phys., 16(3), 1417–1431, https://doi.org/10.5194/acp-16-1417-2016, 2016.

Lane, T. E., Donahue, N. M. and Pandis, S. N.: Effect of NOx on secondary organic aerosol concentrations, Environ. Sci. Technol., 42(16), 6022–6027, https://doi.org/10.1021/es703225a, 2008.

Lannuque, V., Camredon, M., Couvidat, F., Hodzic, A., Valorso, R., Madronich, S., Bessagnet, B. and Aumont, B.: Exploration of the influence of environmental conditions on secondary organic aerosol formation and organic species properties using explicit simulations: development of the VBS-GECKO parameterization, Atmos. Chem. Phys., 18(18), 13411–13428, https://doi.org/10.5194/acp-18-13411-2018, 2018.

Lecœur, E. and Seigneur, C.: Dynamic evaluation of a multi-year model simulation of particulate matter concentrations over Europe, Atmos. Chem. Phys., 13(8), 4319–4337, https://doi.org/10.5194/acp-13-4319-2013, 2013.

Lemaire, V., Coll, I., Couvidat, F., Mouchel-Vallon, C., Seigneur, C. and Siour, G.: Oligomer formation in the troposphere: From experimental knowledge to 3-D modeling, Geosci. Model Dev., 9(4), 1361–1382, https://doi.org/10.5194/gmd-9-1361-2016, 2016.

Lim, S. S., Vos, T., Flaxman, A. D., Danaei, G., Shibuya, K., Adair-Rohani, H., AlMazroa, M. A., Amann, M., Anderson, H. R., Andrews, K. G., Aryee, M., Atkinson, C., Bacchus, L. J., Bahalim, A. N., Balakrishnan, K., Balmes, J., Barker-Collo, S., Baxter, A., Bell, M. L., Blore, J. D., Blyth, F., Bonner, C., Borges, G., Bourne, R., Boussinesq, M., Brauer, M., Brooks, P., Bruce, N. G., Brunekreef, B., Bryan-Hancock, C., Bucello, C., Buchbinder, R., Bull, F., Burnett, R. T., Byers, T. E., Calabria, B., Carapetis, J., Carnahan, E., Chafe, Z., Charlson, F., Chen, H., Chen, J. S., Cheng, A. T.-A., Child, J. C., Cohen, A., Colson, K. E., Cowie, B. C., Darby, S., Darling, S., Davis, A., Degenhardt, L., Dentener, F., Des Jarlais, D. C., Devries, K., Dherani, M., Ding, E. L., Dorsey, E. R., Driscoll, T., Edmond, K., Ali, S. E., Engell, R. E., Erwin, P. J., Fahimi, S., Falder, G., Farzadfar, F., Ferrari, A., Finucane, M. M., Flaxman, S., Fowkes, F. G. R., Freedman, G., Freeman, M. K., Gakidou, E., Ghosh, S., Giovannucci, E., Gmel, G., Graham, K., Grainger, R., Grant, B., Gunnell, D., Gutierrez, H. R., Hall, W., Hoek, H. W., Hogan, A., Hosgood, H. D., Hoy, D., Hu, H., Hubbell, B. J., Hutchings, S. J., Ibeanusi, S. E., Jacklyn, G. L., Jasrasaria, R., Jonas, J. B., Kan, H., Kanis, J. A., Kassebaum, N., Kawakami, N., Khang, Y.-H., Khatibzadeh, S., Khoo, J.-P., et al.: A comparative risk assessment of burden of disease and injury attributable to 67 risk factors and risk factor clusters in 21 regions, 1990–2010: a systematic analysis for the Global Burden of Disease Study 2010, Lancet, 380(9859), 2224–2260, https://doi.org/10.1016/S0140-6736(12)61766-8, 2012.

Louvaris, E. E., Karnezi, E., Kostenidou, E., Kaltsonoudis, C. and Pandis, S. N.: Estimation of the volatility distribution of organic aerosol combining thermodenuder and isothermal dilution measurements, Atmos. Meas. Tech., 10(10), 3909–3918, https://doi.org/10.5194/amt-10-3909-2017, 2017.

Lu, Q., Zhao, Y. and Robinson, A. L.: Comprehensive organic emission profiles for gasoline, diesel, and gas-turbine engines including intermediate and semi-volatile organic compound emissions, Atmos. Chem. Phys., 18(23), 17637–17654, https://doi.org/10.5194/acp-18-17637-2018, 2018.

Mailler, S., Menut, L., Khvorostyanov, D., Valari, M., Couvidat, F., Siour, G., Turquety, S., Briant, R., Tuccella, P., Bessagnet, B., Colette, A., Létinois, L., Markakis, K. and Meleux, F.: CHIMERE-2017: From urban to hemispheric chemistry-transport modeling, Geosci. Model Dev., 10(6), 2397–2423, https://doi.org/10.5194/gmd-10-2397-2017, 2017.

Matsunaga, A. and Ziemann, P. J.: Aerosol Science and Technology Gas-Wall Partitioning of Organic Compounds in a Teflon Film Chamber and Potential Effects on Reaction Product and Aerosol Yield Measurements Gas-Wall Partitioning of Organic Compounds in a Teflon Film Chamber and Potential E, Aerosol Sci. Technol., 4410(44), https://doi.org/10.1080/02786826.2010.501044, 2010.

5   May, A. A., Presto, A. A., Hennigan, C. J., Nguyen, N. T., Gordon, T. D. and Robinson, A. L.: Gas-particle partitioning of primary organic aerosol emissions: (1) Gasoline vehicle exhaust, Atmos. Environ., 77, 128–139, https://doi.org/10.1016/j.atmosenv.2013.04.060, 2013a.

May, A. A., Presto, A. A., Hennigan, C. J., Nguyen, N. T., Gordon, T. D. and Robinson, A. L.: Gas-particle partitioning of primary organic aerosol emissions: (2) diesel vehicles, Environ. Sci. Technol., 47(15), 8288–8296,
10 https://doi.org/10.1021/es400782j, 2013b.

May, A. A., Levin, E. J. T., Hennigan, C. J., Riipinen, I., Lee, T., Collett, J. L., Jimenez, J. L., Kreidenweis, S. M. and Robinson, A. L.: Gas-particle partitioning of primary organic aerosol emissions: 3. Biomass burning, J. Geophys. Res. Atmos., 118(19), 11327–11338, https://doi.org/10.1002/jgrd.50828, 2013c.

McMurry, P. H. and Grosjean, D.: Gas and aerosol wall losses in Teflon film smog chambers, Environ. Sci. Technol.,
15 19(12), 1176–1182, https://doi.org/10.1021/es00142a006, 1985.

Menut, L., Bessagnet, B., Khvorostyanov, D., Beekmann, M., Blond, N., Colette, A., Coll, I., Curci, G., Foret, G., Hodzic, A., Mailler, S., Meleux, F., Monge, J.-L., Pison, I., Siour, G., Turquety, S., Valari, M., Vautard, R. and Vivanco, M. G.: CHIMERE 2013: a model for regional atmospheric composition modelling, Geosci. Model Dev., 6(4), 981–1028, https://doi.org/10.5194/gmd-6-981-2013, 2013.

20 Mircea, M., Bessagnet, B., D'Isidoro, M., Pirovano, G., Aksoyoglu, S., Ciarelli, G., Tsyro, S., Manders, A., Bieser, J., Stern, R., Vivanco, M. G., Cuvelier, C., Aas, W., Prévôt, A. S. H., Aulinger, A., Briganti, G., Calori, G., Cappelletti, A., Colette, A., Couvidat, F., Fagerli, H., Finardi, S., Kranenburg, R., Rouïl, L., Silibello, C., Spindler, G., Poulain, L., Herrmann, H., Jimenez, J. L., Day, D. A., Tiitta, P. and Carbone, S.: EURODELTA III exercise: An evaluation of air quality models' capacity to reproduce the carbonaceous aerosol, Atmos. Environ. X, 2, 100018, https://doi.org/10.1016/j.aeaoa.2019.100018,
25 2019.

Murphy, B. N., Woody, M. C., Jimenez, J. L., Carlton, A. M. G., Hayes, P. L., Liu, S., Ng, N. L., Russell, L. M., Setyan, A., Xu, L., Young, J., Zaveri, R. A., Zhang, Q. and Pye, H. O. T.: Semivolatile POA and parameterized total combustion SOA in CMAQv5.2: Impacts on source strength and partitioning, Atmos. Chem. Phys., 17(18), 11107–11133, https://doi.org/10.5194/acp-17-11107-2017, 2017.

30 Ng, N. L., Chhabra, P. S., Chan, a. W. H., Surratt, J. D., Kroll, J. H., Kwan, a. J., McCabe, D. C., Wennberg, P. O., Sorooshian, A., Murphy, S. M., Dalleska, N. F., Flagan, R. C. and Seinfeld, J. H.: Effect of NOx level on secondary organic aerosol (SOA) formation from the photooxidation of terpenes, Atmos. Chem. Phys., 7(4), 5159–5174, https://doi.org/10.5194/acpd-7-10131-2007, 2007.

Ntziachristos, L., Gkatzoflias, D., Kouridis, C. and Samaras, Z.: COPERT: A European Road Transport Emission Inventory Model, edited by I. N. Athanasiadis, A. E. Rizzoli, P. A. Mitkas, and J. M. Gómez, pp. 491–504, Springer, Berlin, Heidelberg., 2009.

Odum, J. R., Hoffmann, T., Bowman, F., Collins, D., Flagan, R. C. and Seinfeld, J. H.: Gas particle partitioning and
5   secondary organic aerosol yields, Environ. Sci. Technol., 30(8), 2580–2585, https://doi.org/10.1021/es950943+, 1996.

Ots, R., Young, D. E., Vieno, M., Xu, L., Dunmore, R. E., Allan, J. D., Coe, H., Williams, L. R., Herndon, S. C., Ng, N. L., Hamilton, J. F., Bergström, R., Di Marco, C., Nemitz, E., Mackenzie, I. A., Kuenen, J. J. P., Green, D. C., Reis, S. and Heal, M. R.: Simulating secondary organic aerosol from missing diesel-related intermediate-volatility organic compound emissions during the Clean Air for London (ClearfLo) campaign, Atmos. Chem. Phys., 16(10), 6453–6473,
10 https://doi.org/10.5194/acp-16-6453-2016, 2016.

Pandis, S. N., Wexler, A. S. and Seinfeld, J. H.: Secondary organic aerosol formation and transport — II. Predicting the ambient secondary organic aerosol size distribution, Atmos. Environ., 27(15), 2403–2416, https://doi.org/10.1016/0960-1686(93)90408-Q, 1993.

Passant, N. R.: Speciation of UK emissions of non-methane volatile organic compounds, AEA Technol. Rep. ENV-0545,
15 (1), 1–289, 2002.

Paulot, F., Crounse, J. D., Kjaergaard, H. G., Kurten, A., St. Clair, J. M., Seinfeld, J. H. and Wennberg, P. O.: Unexpected Epoxide Formation in the Gas-Phase Photooxidation of Isoprene, Science (80-.)., 325(5941), 730–733, https://doi.org/10.1126/science.1172910, 2009.

Petetin, H., Beekmann, M., Sciare, J., Bressi, M., Rosso, A., Sanchez, O. and Ghersi, V.: A novel model evaluation approach
20 focusing on local and advected contributions to urban PM2.5 levels - Application to Paris, France, Geosci. Model Dev., 7(4), 1483–1505, https://doi.org/10.5194/gmd-7-1483-2014, 2014.

Pun, B. K., Griffin, R. J., Seigneur, C. and Seinfeld, J. H.: Secondary organic aerosol 2. Thermodynamic model for gas/particle partitioning of molecular constituents, J. Geophys. Res. Atmos., 107(17), AAC4/1-AAC4/15, https://doi.org/10.1029/2001JD000542, 2002.

25 Pun, B. K., Wu, S. Y., Seigneur, C., Seinfeld, J. H., Griffin, R. J. and Pandis, S. N.: Uncertainties in modeling secondary organic aerosols: Three-dimensional modeling studies in Nashville/Western Tennessee, Environ. Sci. Technol., 37(16), 3647–3661, https://doi.org/10.1021/es0341541, 2003.

Pun, B. K., Seigneur, C., Vijayaraghavan, K., Wu, S. Y., Chen, S. Y., Knipping, E. M. and Kumar, N.: Modeling regional haze in the BRAVO study using CMAQ-MADRID: 1. Model evaluation, J. Geophys. Res. Atmos., 111(6), 1–25,
30 https://doi.org/10.1029/2004JD005608, 2006a.

Pun, B. K., Seigneur, C. and Lohman, K.: Modeling secondary organic aerosol formation via multiphase partitioning with molecular data, Environ. Sci. Technol., 40(15), 4722–4731, https://doi.org/10.1021/es0522736, 2006b.

Pye, H. O. T., Zuend, A., Fry, J. L., Isaacman-VanWertz, G., Capps, S. L., Appel, K. W., Foroutan, H., Xu, L., Ng, N. L. and Goldstein, A. H.: Coupling of organic and inorganic aerosol systems and the effect on gas&amp;ndash;particle partitioning in the southeastern US, Atmos. Chem. Phys., 18(1), 357–370, https://doi.org/10.5194/acp-18-357-2018, 2018.

Robinson, A. L., Donahue, N. M., Shrivastava, M. K., Weitkamp, E. A., Sage, A. M., Grieshop, A. P., Lane, T. E., Pierce, J. R. and Pandis, S. N.: Rethinking Organic Aerosols: Semivolatile Emissions and Photochemical Aging, Science (80-.)., 315(5816), 1259–1262, https://doi.org/10.1126/science.1133061, 2007.

Rudich, Y., Donahue, N. M. and Mentel, T. F.: Aging of Organic Aerosol: Bridging the Gap Between Laboratory and Field Studies, Annu. Rev. Phys. Chem., 58(1), 321–352, https://doi.org/10.1146/annurev.physchem.58.032806.104432, 2007.

Sarwar, G., Godowitch, J., Henderson, B. H., Fahey, K., Pouliot, G., Hutzell, W. T., Mathur, R., Kang, D., Goliff, W. S. and Stockwell, W. R.: A comparison of atmospheric composition using the Carbon Bond and Regional Atmospheric Chemistry Mechanisms, Atmos. Chem. Phys., 13(19), 9695–9712, https://doi.org/10.5194/acp-13-9695-2013, 2013.

Schauer, J. J., Kleeman, M. J., Cass, G. R. and Simoneit, B. R. T.: Measurement of emissions from air pollution sources. 2. C1 through C30 organic compounds from medium duty diesel trucks, Environ. Sci. Technol., 33(10), 1578–1587, https://doi.org/10.1021/es980081n, 1999.

Schauer, J. J., Kleeman, M. J., Cass, G. R. and Simoneit, B. R. T.: Measurement of emissions from air pollution sources. 5. C1-C32 organic compounds from gasoline-powered motor vehicles., Environ. Sci. Technol., 36(6), 1169–1180, https://doi.org/10.1021/es0108077, 2002.

Schell, B., Ackermann, I. J., Hass, H., Binkowski, F. S. and Ebel, A.: Modeling the formation of secondary organic aerosol within a comprehensive air quality model system, J. Geophys. Res. Atmos., 106(D22), 28275–28293, https://doi.org/10.1029/2001JD000384, 2001.

Schmidt, H., Derognat, C., Vautard, R. and Beekmann, M.: A comparison of simulated and observed ozone mixing ratios for the summer of 1998 in Western Europe, Atmos. Environ., 35(36), 6277–6297, https://doi.org/10.1016/S1352-2310(01)00451-4, 2001.

Shiraiwa, M., Zuend, A., Bertram, A. K. and Seinfeld, J. H.: Gas–particle partitioning of atmospheric aerosols: interplay of physical state, non-ideal mixing and morphology, Phys. Chem. Chem. Phys., 15(27), 11441, https://doi.org/10.1039/c3cp51595h, 2013.

Solazzo, E., Bianconi, R., Pirovano, G., Matthias, V., Vautard, R., Moran, M. D., Wyat Appel, K., Bessagnet, B., Brandt, J., Christensen, J. H., Chemel, C., Coll, I., Ferreira, J., Forkel, R., Francis, X. V, Grell, G., Grossi, P., Hansen, A. B., Miranda, A. I., Nopmongcol, U., Prank, M., Sartelet, K. N., Schaap, M., Silver, J. D., Sokhi, R. S., Vira, J., Werhahn, J., Wolke, R., Yarwood, G., Zhang, J., Rao, S. T. and Galmarini, S.: Operational model evaluation for particulate matter in Europe and North America in the context of AQMEII, Atmos. Environ., 53, 75–92, https://doi.org/10.1016/j.atmosenv.2012.02.045, 2012.

29

Surratt, J. D., Chan, A. W. H., Eddingsaas, N. C., Chan, M., Loza, C. L., Kwan, A. J., Hersey, S. P., Flagan, R. C., Wennberg, P. O. and Seinfeld, J. H.: Reactive intermediates revealed in secondary organic aerosol formation from isoprene, Proc. Natl. Acad. Sci., 107(15), 6640–6645, https://doi.org/10.1073/pnas.0911114107, 2010.

Tørseth, K., Aas, W., Breivik, K., Fjeraa, A. M., Fiebig, M., Hjellbrekke, A. G., Lund Myhre, C., Solberg, S. and Yttri, K. E.: Introduction to the European Monitoring and Evaluation Programme (EMEP) and observed atmospheric composition change during 1972-2009, Atmos. Chem. Phys., 12(12), 5447–5481, https://doi.org/10.5194/acp-12-5447-2012, 2012.

Trump, E. R. and Donahue, N. M.: Oligomer formation within secondary organic aerosols: equilibrium and dynamic considerations, Atmos. Chem. Phys., 14(7), 3691–3701, https://doi.org/10.5194/acp-14-3691-2014, 2014.

Tsigaridis, K., Daskalakis, N., Kanakidou, M., Adams, P. J., Artaxo, P., Bahadur, R., Balkanski, Y., Bauer, S. E., Bellouin, N., Benedetti, A., Bergman, T., Berntsen, T. K., Beukes, J. P., Bian, H., Carslaw, K. S., Chin, M., Curci, G., Diehl, T., Easter, R. C., Ghan, S. J., Gong, S. L., Hodzic, A., Hoyle, C. R., Iversen, T., Jathar, S., Jimenez, J. L., Kaiser, J. W., Kirkeväg, A., Koch, D., Kokkola, H., H Lee, Y., Lin, G., Liu, X., Luo, G., Ma, X., Mann, G. W., Mihalopoulos, N., Morcrette, J. J., Müller, J. F., Myhre, G., Myriokefalitakis, S., Ng, N. L., O'donnell, D., Penner, J. E., Pozzoli, L., Pringle, K. J., Russell, L. M., Schulz, M., Sciare, J., Seland, Shindell, D. T., Sillman, S., Skeie, R. B., Spracklen, D., Stavrakou, T., Steenrod, S. D., Takemura, T., Tiitta, P., Tilmes, S., Tost, H., Van Noije, T., Van Zyl, P. G., Von Salzen, K., Yu, F., Wang, Z., Wang, Z., Zaveri, R. A., Zhang, H., Zhang, K., Zhang, Q. and Zhang, X.: The AeroCom evaluation and intercomparison of organic aerosol in global models, Atmos. Chem. Phys., 14(19), 10845–10895, https://doi.org/10.5194/acp-14-10845-2014, 2014.

Tsimpidi, a. P., Karydis, V. a., Zavala, M., Lei, W., Molina, L., Ulbrich, I. M., Jimenez, J. L. and Pandis, S. N.: Evaluation of the volatility basis-set approach for the simulation of organic aerosol formation in the Mexico City metropolitan area, Atmos. Chem. Phys., 9(3), 13693–13737, https://doi.org/10.5194/acpd-9-13693-2009, 2010.

Valorso, R., Aumont, B., Camredon, M., Raventos-Duran, T., Mouchel-Vallon, C., Ng, N. L., Seinfeld, J. H., Lee-Taylor, J. and Madronich, S.: Explicit modelling of SOA formation from α-pinene photooxidation: Sensitivity to vapour pressure estimation, Atmos. Chem. Phys., 11(14), 6895–6910, https://doi.org/10.5194/acp-11-6895-2011, 2011.

Vestreng, V.: Review and revision, emission data reported to CLRTAP, , (July), 134 [online] Available from: http://tfeip-secretariat.org/assets/Meetings/Documents/Previous-Meetings/Poland-Sept-2003/ReviewandrevisionMSCWStatusReport2003.pdf, 2003.

Volkamer, R., Jimenez, J. L., San Martini, F., Dzepina, K., Zhang, Q., Salcedo, D., Molina, L. T., Worsnop, D. R. and Molina, M. J.: Secondary organic aerosol formation from anthropogenic air pollution: Rapid and higher than expected, Geophys. Res. Lett., 33(17), L17811, https://doi.org/10.1029/2006GL026899, 2006.

Wesely, M. L.: Parameterization of surface resistances to gaseous dry deposition in regional-scale numerical models, Atmos. Environ., 23(6), 1293–1304, https://doi.org/10.1016/0004-6981(89)90153-4, 1989.

WHO Regional Office for Europe OECD: Economic cost of the health impact of air pollution in Europe: Clean air, health and wealth., Eur. Environ. Heal. Process., 1–54, 2015.

Woody, M. C., West, J. J., Jathar, S. H., Robinson, A. L. and Arunachalam, S.: Estimates of non-traditional secondary organic aerosols from aircraft SVOC and IVOC emissions using CMAQ, Atmos. Chem. Phys., 15(12), 6929–6942, https://doi.org/10.5194/acp-15-6929-2015, 2015.

Woody, M. C., Baker, K. R., Hayes, P. L., Jimenez, J. L., Koo, B. and Pye, H. O. T.: Understanding sources of organic aerosol during CalNex-2010 using the CMAQ-VBS, Atmos. Chem. Phys., 16(6), 4081–4100, https://doi.org/10.5194/acp-16-4081-2016, 2016.

Zhao, Y., Nguyen, N. T., Presto, A. A., Hennigan, C. J., May, A. A. and Robinson, A. L.: Intermediate Volatility Organic Compound Emissions from On-Road Diesel Vehicles: Chemical Composition, Emission Factors, and Estimated Secondary Organic Aerosol Production, Environ. Sci. Technol., 49(19), 11516–11526, https://doi.org/10.1021/acs.est.5b02841, 2015.

Zhao, Y., Nguyen, N. T., Presto, A. A., Hennigan, C. J., May, A. A. and Robinson, A. L.: Intermediate Volatility Organic Compound Emissions from On-Road Gasoline Vehicles and Small Off-Road Gasoline Engines, Environ. Sci. Technol., 50(8), 4554–4563, https://doi.org/10.1021/acs.est.5b06247, 2016.

Zhu, S., Sartelet, K. N., Healy, R. M. and Wenger, J. C.: Simulation of particle diversity and mixing state over Greater Paris: a model–measurement inter-comparison, Faraday Discuss., 189(189), 547–566, https://doi.org/10.1039/C5FD00175G, 2016a.

Zhu, S., Sartelet, K., Zhang, Y. and Nenes, A.: Three-dimensional modeling of the mixing state of particles over Greater Paris, J. Geophys. Res. Atmos., 121(10), 5930–5947, https://doi.org/10.1002/2015JD024241, 2016b.

Table 1 – List of the VBS-GECKO species and associated properties.

Species	Partition[b]	MW (g.mol^{-1})	P$^{sat}_{298K}$ (atm)	H$^{eff}_{298K}$ (mol.L^{-1}.atm^{-1})	ΔH_{vap} (kJ.mol^{-1})
α-pinene		136	4.47×10^{-3}	1.70×10^{-2}	46
β-pinene		136	4.79×10^{-3}	1.70×10^{-2}	45
Limonene		136	4.57×10^{-3}	1.70×10^{-2}	46
Benzene		78	6.61×10^{-2}	0.21	36
Toluene		92	2.14×10^{-2}	0.18	40
O-xylene		106	7.24×10^{-3}	0.25	45
M-xylene		106	5.75×10^{-3}	0.16	45
P-xylene		106	7.24×10^{-3}	0.17	45
decane		142	1.90×10^{-3}	1.41×10^{-4}	50
Tetradecane	*	198	3.63×10^{-5}	7.94×10^{-5}	66
Octadecane	*	254	7.76×10^{-7}	2.57×10^{-5}	83
Docosane	*	310	1.66×10^{-8}	8.51×10^{-6}	100
Hexacosane	*	366	3.39×10^{-10}	2.82×10^{-6}	118
Decene		140	2.04×10^{-3}	1.00×10^{-3}	50
Tetradecene	*	196	3.98×10^{-5}	3.31×10^{-4}	66
Octadecene	*	253	8.71×10^{-7}	1.10×10^{-4}	82
Docosene	*	308	1.91×10^{-8}	3.63×10^{-5}	99
Hexacosene	*	364	4.07×10^{-10}	1.20×10^{-5}	117
VB$_{k,1}$[a]	*	210	3.16×10^{-7}	1.0×10^{6}	90
VB$_{k,2}$[a]	*	240	1.0×10^{-8}	1.0×10^{7}	105
VB$_{k,3}$[a]	*	270	1.0×10^{-9}	1.0×10^{8}	115
VB$_{k,4}$[a]	*	300	1.0×10^{-10}	1.0×10^{9}	125
VB$_{k,5}$[a]	*	330	1.0×10^{-11}	1.0×10^{10}	135
VB$_{k,6}$[a]	*	360	1.0×10^{-12}	1.0×10^{11}	145
VB$_{k,7}$[a]	*	390	1.0×10^{-14}	1.0×10^{12}	165

[a] Properties of the bins do not depend on the precursor k (see Lannuque et al., 2018)
[b] Gas/particle partitioning is implemented in CHIMERE for species with a * only

Table 2 – Distribution of the NMVOC emission in the VBS-GECKO species.

VBS-GECKO	Emitted NMVOC in CHIMERE (Passant, 2002)
Decane	C10 alkanes; C10 cycloalkanes; 75% of C11 alkanes; 50% of C12 alkanes; 25% of C13 alkanes
Tetradecane	25% of C11 alkanes; 50% of C12 alkanes; 75% of C13 alkanes
Decene	C10 alkenes
Benzene	Benzene
Toluene	25% of C9, C10, C13 and unspeciated aromatic hydrocarbons, ethylbenzene, isopropylbenzene, propylbenzene, phenol, toluene and styrene
O-xylene	25% of C9, C10, C13 and unspeciated aromatic hydrocarbons; 2-ethyltoluene; indan; 33% of ethyltoluene; 33% of methylpropylbenzene; o-xylene
M-xylene	25% of C9, C10, C13 and unspeciated aromatic hydrocarbons, tetramethylbenzene; trimethylbenzene; 1-methyl-3-isopropylbenzene; 3-ethyltoluene; ethyldimethylbenzene; 33% of ethyltoluene; 33% of methylpropylbenzene; m-xylene
P-xylene	25% of C9, C10, C13 and unspeciated aromatic hydrocarbons; 1-methyl-4-isopropylbenzene; 4-ethyltoluene; 33% of ethyltoluene; 33% of methylpropylbenzene; p-xylene

Table 3 – Statistical results calculated on daily averaged concentrations for the ref-VBS-GECKO simulations and differences between ref-VBS-GECKO and H^{2}O statistical indicators.

	Observations		VBS-GECKO results					Differences with H^{2}O results				
	Number	Mean	Mean	RMSE	r	MFB	MFE	Δ mean	Δ RMSE	Δ r	Δ MFB	Δ MFE
	-	(μg.m^{-3})	(μg.m^{-3})	(μg.m^{-3})	-	-	-	(%)	(%)	-	(dist from 0)	-
PM$_{2.5}$	2002	9.07	7.65	6.14	0.42	-0.09	0.37	+5.52	-1.76	+0.01	-0.05	-0.01
OM$_{PM1}$	237	3.24	1.93	2.28	0.79	-0.47	0.57	+31.3	-11.6	-0.04	-0.25	-0.17
OC$_{PM2.5}$	235	2.52	2.59	1.75	0.57	-0.16	0.51	+15.6	+5.42	+0.02	-0.17	-0.08

5

Table 4 – Statistical results calculated on daily averaged concentrations simulated with the various model configurations and differences with the ref-VBS-GECKO configuration statistical indicators given Table 3.

Model configuration		Sensitivity test results					Differences to ref-VBS-GECKO results				
		Mean	RMSE	r	MFB	MFE	Δ mean	Δ RMSE	Δ r	Δ MFB	Δ MFE
		(μg.m^{-3})	(μg.m^{-3})	-	-	-	(%)	(%)	-	(dist from 0)	-
hydro-VBS-GECKO	OM$_{PM1}$	1.93	2.28	0.79	-0.47	0.57	0.00	0.00	0.00	0.00	0.00
	OC$_{PM2.5}$	2.59	1.75	0.57	-0.16	0.51	0.00	0.00	0.00	0.00	0.00
hydro-VBS-GECKO-high	OM$_{PM1}$	2.07	2.17	0.79	-0.41	0.52	+7.43	-4.58	0.00	-0.06	-0.05
	OC$_{PM2.5}$	2.71	1.73	0.57	-0.11	0.48	+4.80	-0.65	0.00	-0.05	-0.03
k$_{OH}$-VBS-GECKO-low	OM$_{PM1}$	1.87	2.32	0.78	-0.49	0.59	-2.70	+1.90	-0.01	+0.02	+0.02
	OC$_{PM2.5}$	2.52	1.73	0.57	-0.19	0.53	-2.40	-0.65	0.00	+0.03	+0.02
k$_{OH}$-VB-GECKO-high	OM$_{PM1}$	2.02	2.21	0.79	-0.43	0.54	+4.72	-2.67	0.00	-0.04	-0.03
	OC$_{PM2.5}$	2.70	1.76	0.57	-0.12	0.49	+4.32	+0.65	0.00	-0.04	-0.02
RRR-VBS-GECKO-low	OM$_{PM1}$	2.11	2.13	0.80	-0.41	0.52	+9.45	-6.48	0.01	-0.06	-0.05
	OC$_{PM2.5}$	2.82	1.81	0.57	-0.08	0.48	+9.13	+3.92	0.00	-0.08	-0.03
RRR-VBS-GECKO-high	OM$_{PM1}$	1.73	2.42	0.78	-0.54	0.64	-10.1	+6.48	-0.01	+0.07	+0.07
	OC$_{PM2.5}$	2.36	1.72	0.56	-0.25	0.56	-8.65	-1.30	-0.01	+0.09	+0.05
P^{sat}-VBS-GECKO-low	OM$_{PM1}$	2.42	1.92	0.80	-0.31	0.44	+25.6	-15.6	+0.01	-0.16	-0.13
	OC$_{PM2.5}$	3.17	1.99	0.58	0.02	0.45	+22.5	+13.7	+0.01	-0.18	-0.06
P^{sat}-VBS-GECKO-high	OM$_{PM1}$	1.47	2.63	0.76	-0.65	0.73	-23.6	+15.6	-0.03	+0.18	+0.16
	OC$_{PM2.5}$	2.07	1.76	0.56	-0.36	0.63	-19.7	+0.65	-0.01	+0.20	+0.12

10

Table 5 – Distribution of the VBS-GECKO surrogate species for IVOC emission in the various model configurations.

Model configuration	Species			
	C14	C18	C22	C26
IVOC$_{150POA}$	105 % of POA	80 % POA	40 % of POA	25 % of POA
IVOC$_{4VOC}$	2.8 % of NMVOCs	35 % of POA + 1,2 % of NMVOCs	40 % of POA	25 % of POA
IVOC$_{16VOC}$	11.2 % of NMVOCs	35 % of POA + 4.8 % of NMVOCs	40 % of POA	25 % of POA
IVOC$_{30VOC}$	21 % of NMVOCs	35 % of POA + 9 % of NMVOCs	40 % of POA	25 % of POA
IVOC$_{65VOC}$	45.5 % of NMVOCs	35 % of POA + 19.5 % of NMVOCs	40 % of POA	25 % of POA

5 **Table 6 – Statistical results calculated on daily averaged concentrations simulated with VBS-GECKO considering IVOC emissions and differences with those of the ref-VBS-GECKO (without IVOCs) from Table 3.**

Model configuration		VBS-GECKO with IVOC results					Differences with ref-VBS-GECKO				
		Mean	RMSE	r	MFB	MFE	Δ Mean	Δ RMSE	Δ r	Δ MFB	Δ MFE
		(µg.m^{-3})	(µg.m^{-3})	-	-	-	%	%	-	(dist from 0)	-
IVOC$_{150POA}$	OM$_{PM1}$	2.02	2.18	0.80	-0.43	0.53	+4.66	-4.38	+0.01	-0.04	-0.04
	OC$_{PM2.5}$	2.72	1.83	0.57	-0.11	0.5	+5.01	+4.57	0.00	-0.05	-0.01
IVOC$_{4VOC}$	OM$_{PM1}$	1.96	2.24	0.79	-0.46	0.56	+1.55	-1.75	0.00	-0.01	-0.01
	OC$_{PM2.5}$	2.64	1.79	0.57	-0.15	0.51	+1.93	+2.28	0.00	-0.01	0.00
IVOC$_{16VOC}$	OM$_{PM1}$	2.01	2.20	0.8	-0.44	0.54	+4.14	-3.50	+0.01	-0.03	-0.03
	OC$_{PM2.5}$	2.73	1.88	0.57	-0.12	0.51	+5.40	+7.42	0.00	-0.04	0.00
IVOC$_{30VOC}$	OM$_{PM1}$	2.06	2.15	0.80	-0.42	0.53	+6.73	-5.70	+0.01	-0.05	-0.04
	OC$_{PM2.5}$	2.84	1.98	0.57	-0.09	0.51	+9.65	+13.1	0.00	-0.07	0.00
IVOC$_{65VOC}$	OM$_{PM1}$	2.18	2.04	0.81	-0.37	0.50	+12.9	-10.5	+0.02	-0.10	-0.07
	OC$_{PM2.5}$	3.10	2.29	0.56	-0.02	0.50	+19.6	+30.8	-0.01	-0.14	-0.01

10
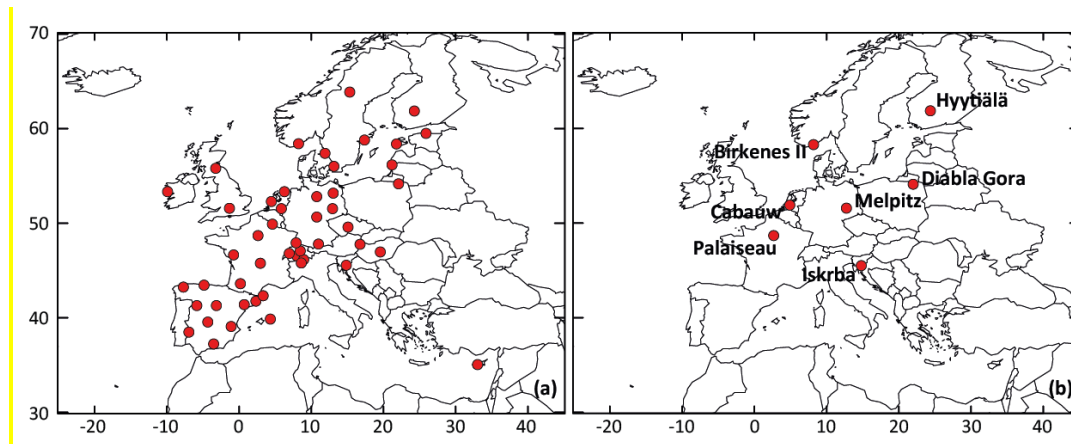
Figure 1 – Location of rural background stations used for (a) the statistical evaluations and (b) time series comparisons.
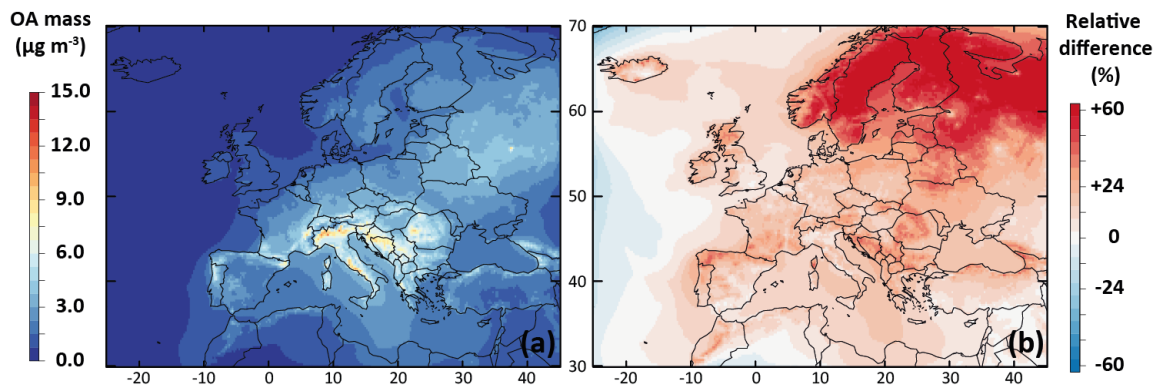
5

10

15

Figure 2 – Mean OA mass concentrations simulated with the ref-VBS-GECKO model configuration over Europe for the July-August 2013 period (a) and relative difference of the simulated mean OA mass concentrations between the ref-VBS-GECKO and the H^2O configuration (b).
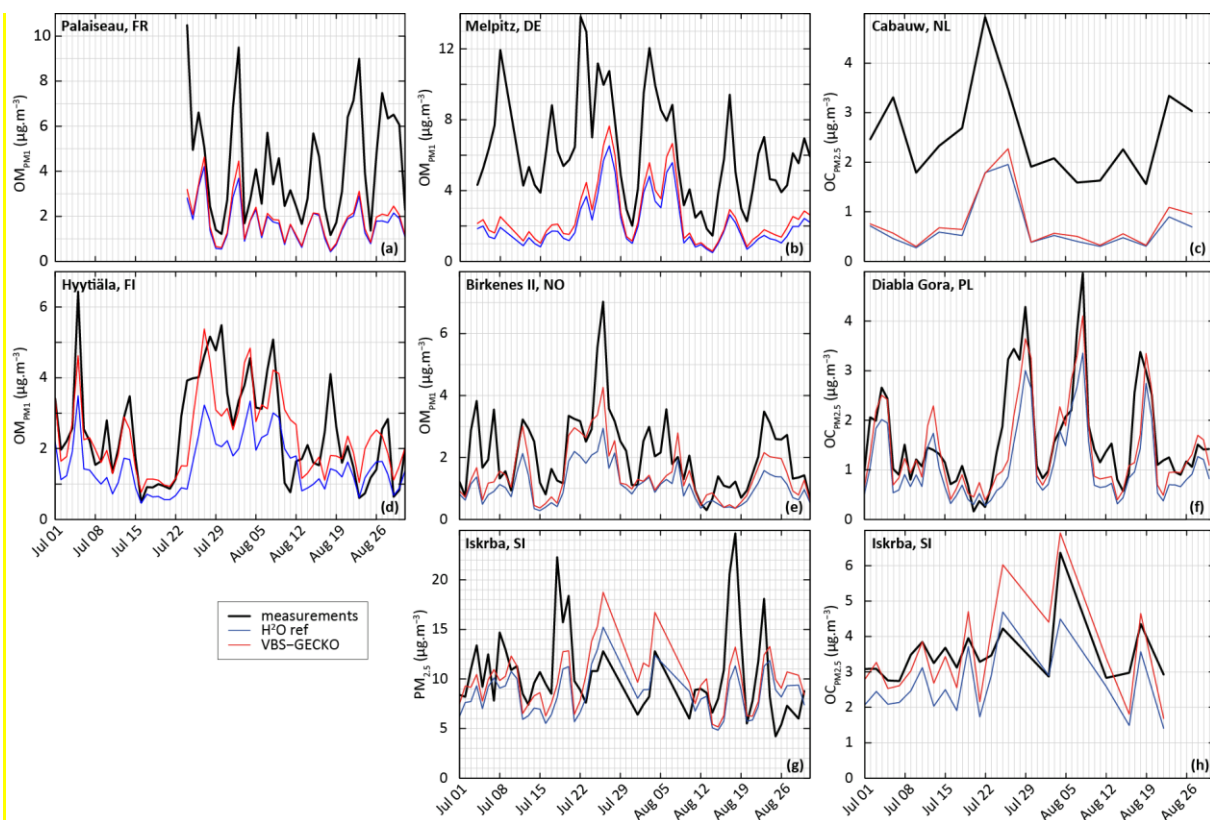

Figure 3 – Measured (black) and simulated (with H^2O in blue and ref-VBS-GECKO in red) temporal evolution of daily averaged OM_{PM1} concentrations (panels a, b, d and e) $OC_{PM2.5}$ concentrations (panels c, f and h) and $PM_{2.5}$ concentrations (panel g). Top panels are for stations influenced by anthropogenic sources in France (Palaiseau station, a), Germany (Melpitz station, b) and Netherland (Cabauw station, c), middle panels are stations in remote areas in Finland (Hyytiälä station, d), Norway (Birkenes II station, d) and Poland (Diabla Gora station, e) and bottom panels are for a station located in a remote area in Slovenia (Iskrba, g and h).

36
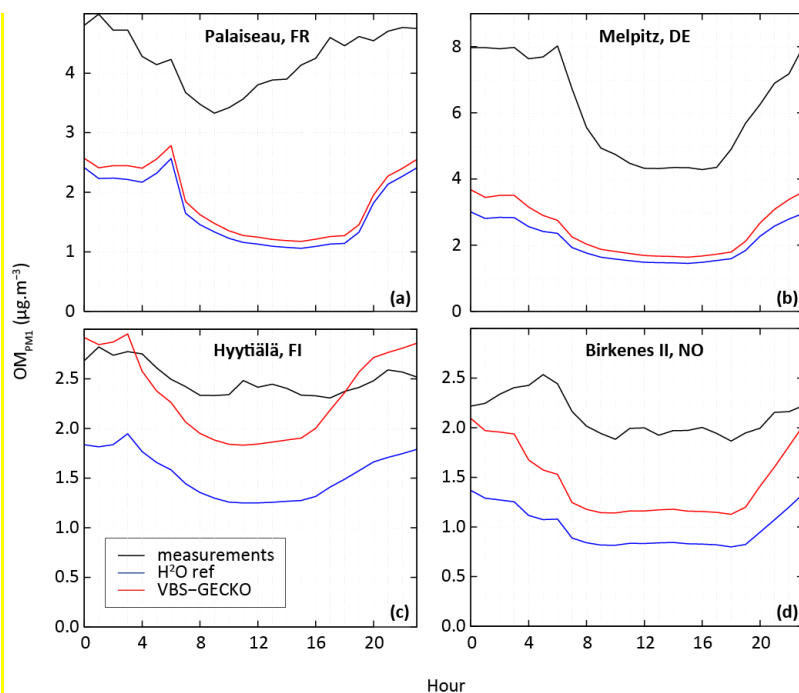
Figure 4 – Measured (black) and simulated mean diurnal profile (in UTC) with the H^{2}O model configuration (blue) and the ref-VBS-GECKO model configuration (red) for OM$_{PM1}$ concentration at stations influenced dominantly by anthropogenic sources (Palaiseau (a) and Melpitz (b)) and by biogenic sources (Hyytiälä (c) and Birkenes II (d)).

5

37
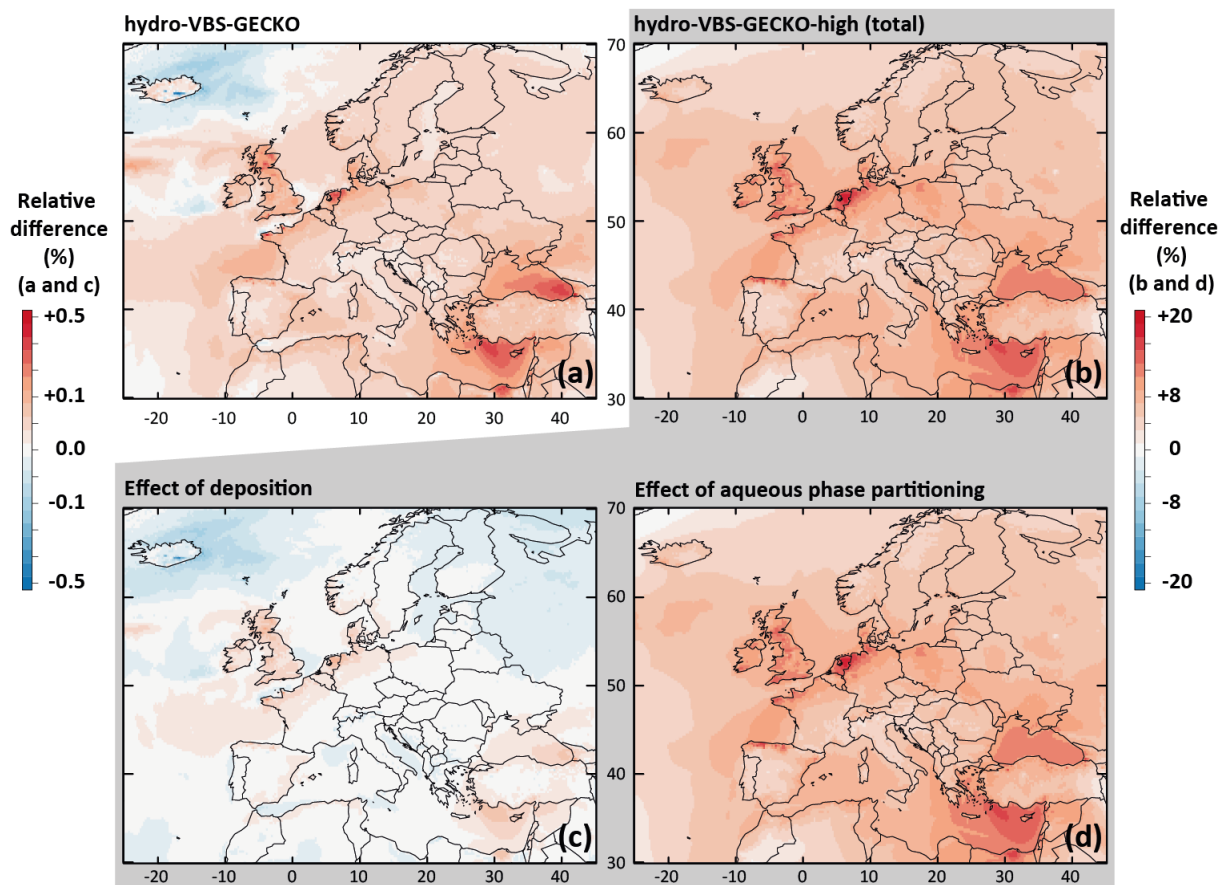
Figure 5 – Relative differences on the simulated mean OA concentrations between (a) the Hydro-VBS-GECKO and the ref-VBS-GECKO and (b) the Hydro-VBS-GECKO-high and the 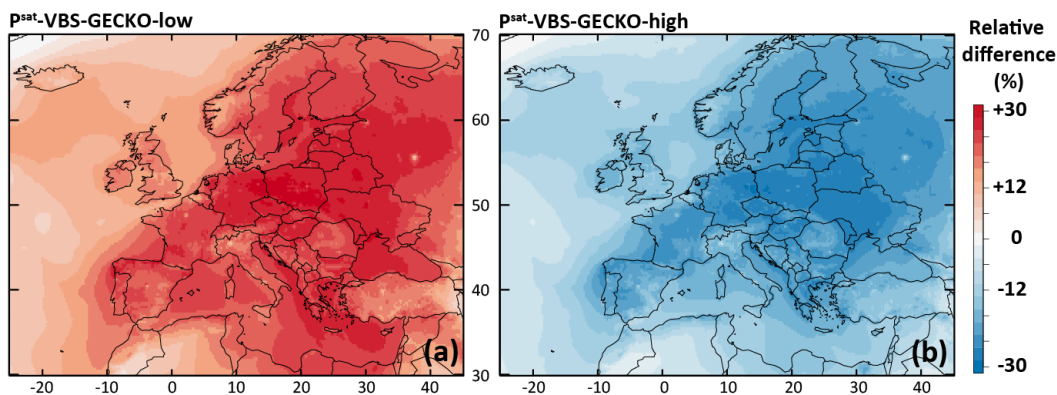ref-VBS-GECKO model configurations for the two-month period. Bottom panels represent relative differences on the simulated mean OA concentrations between the Hydro-VBS-GECKO-high and the ref-VBS-GECKO due to variation in deposition (c) or partitioning (d).
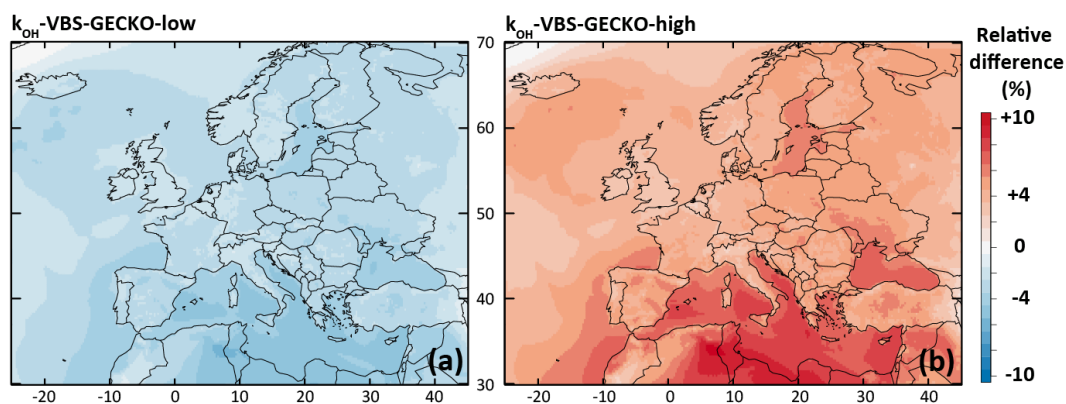
Figure 6 – Relative differences on the simulated mean OA concentrations between (a) the k_{OH}-VBS-GECKO-low and the ref-VBS-GECKO model configurations and (b) the k_{OH}-VBS-GECKO-high and the ref-VBS-GECKO model configurations for the two-month period.
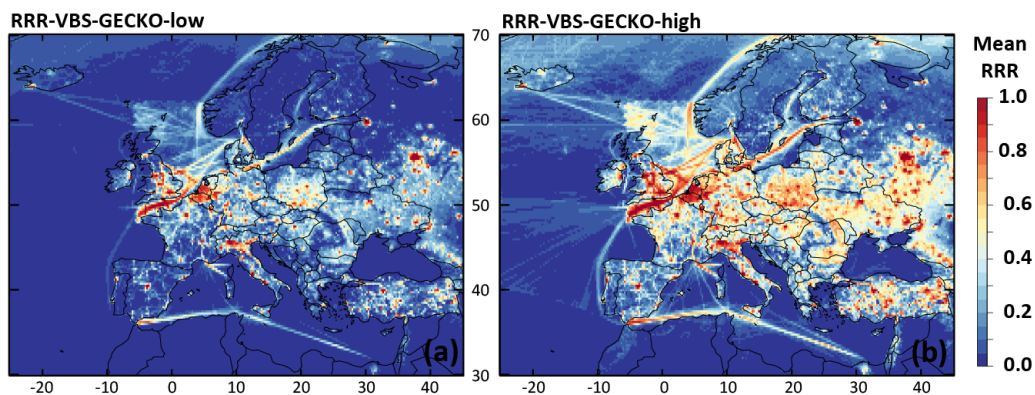
**Figure 7 – Mean RRR over Europe during the two-month period for (a) the RRR-VBS-GECKO-low and (b) the RRR-VBS-GECKO-high model configurations.**
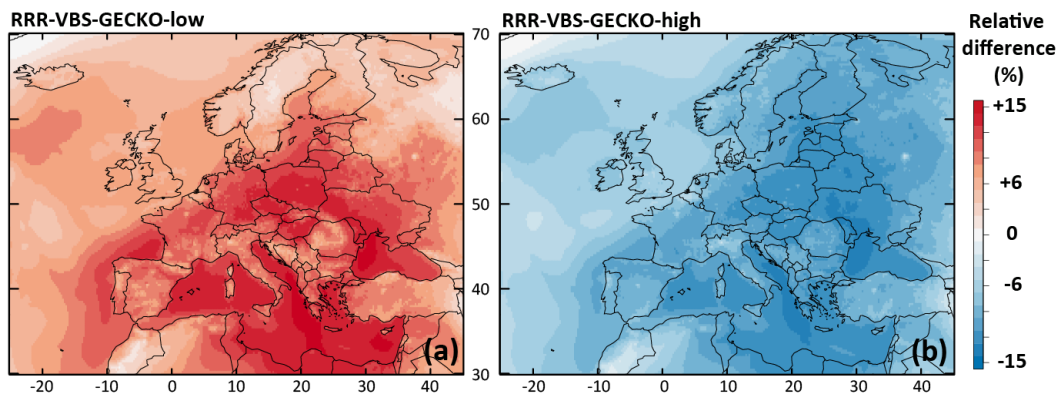
Figure 8 – Relative differences on the simulated mean OA concentrations between (a) the RRR-VBS-GECKO-low and the ref-VBS-GECKO model configurations and (b) between the RRR-VBS-GECKO-high and the ref-VBS-GECKO model configurations for the two-month period.

Figure 9 – Relative difference on the simulated mean OA concentrations between (a) the P^sat-VBS- -low and the ref-VBS-GECKO model configurations and (b) between the P^sat-VBS-GECKO-high and the ref-VBS-GECKO model configurations for the two-month period.

5
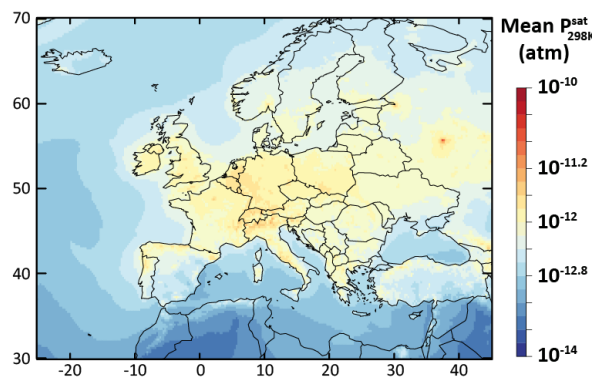
Figure 10 – Simulated average volatility of OA in term of P^{sat}_{298K} upon Europe during the July-August 2013 period for the ref-VBS-GECKO model configuration.
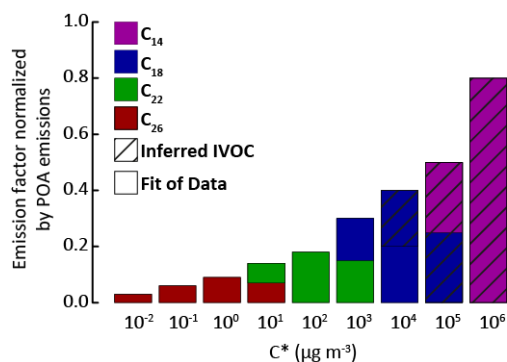
10   **Figure 11 – Distribution of the VBS-GECKO species into the <mark>S/IVOC volatility bins of Robinson et al. (2007)</mark>. Normalized emission factors by POA emissions for IVOCs are used for the IVOC_{150POA} model configuration.**
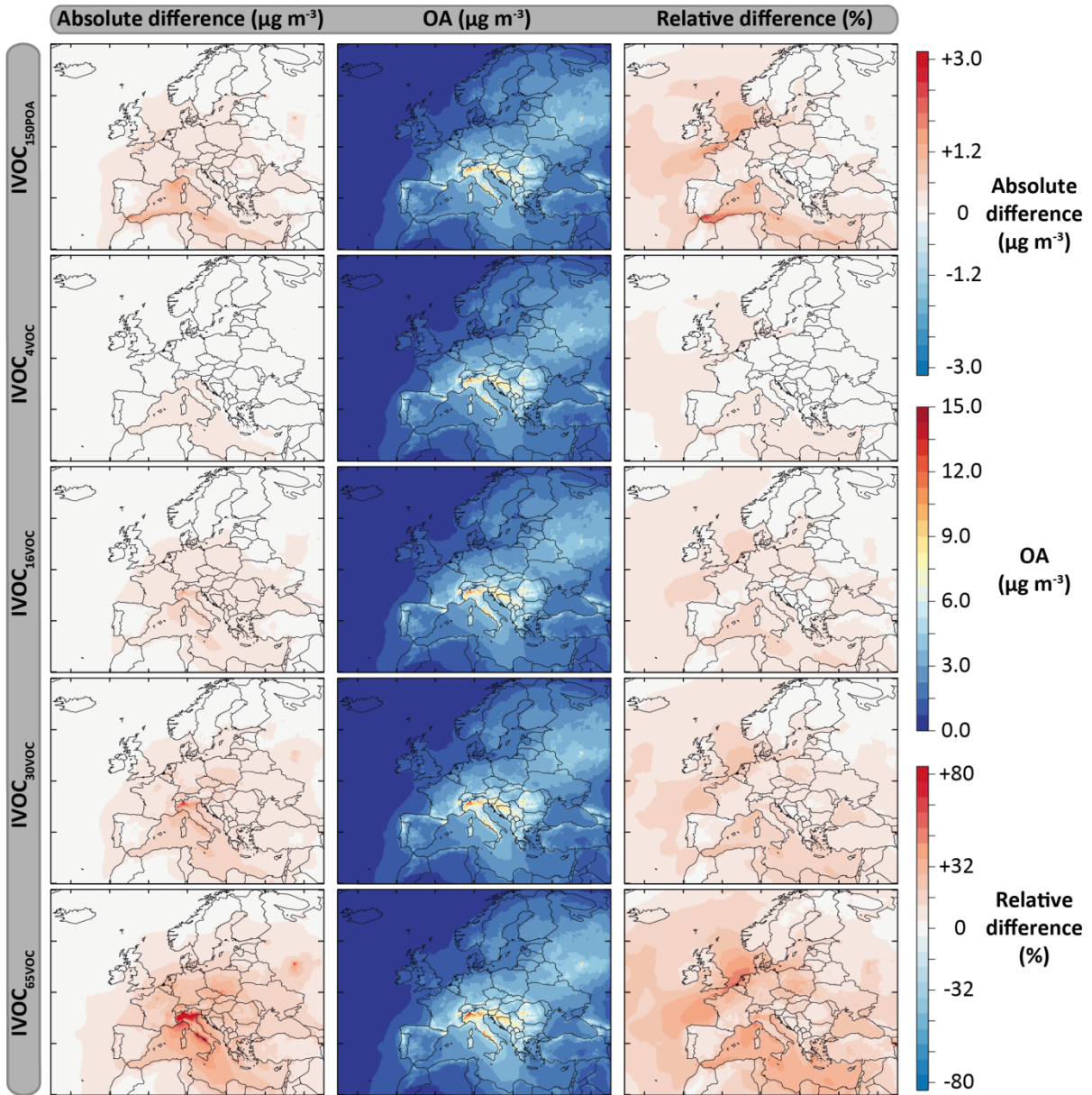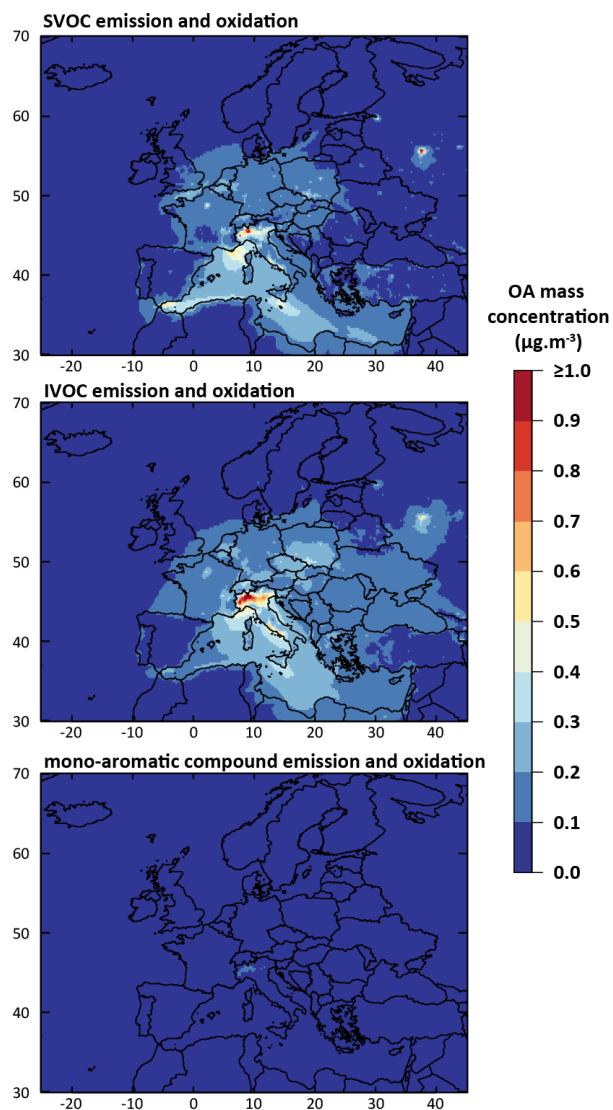
Figure 12 – Mean OA mass concentrations simulated with the model configurations including the IVOC emissions for the July-August 2013 period over Europe (second column), and absolute and relative differences with the ref-VBS-GECKO model configurations (left and right columns respectively). Results are given for the following model configurations: IVOC$_{150POA}$ (first row), IVOC$_{4VOC}$ (second row), IVOC$_{16VOC}$ (third row), IVOC$_{30VOC}$ (fourth row) and IVOC$_{65VOC}$ (fifth row).

41
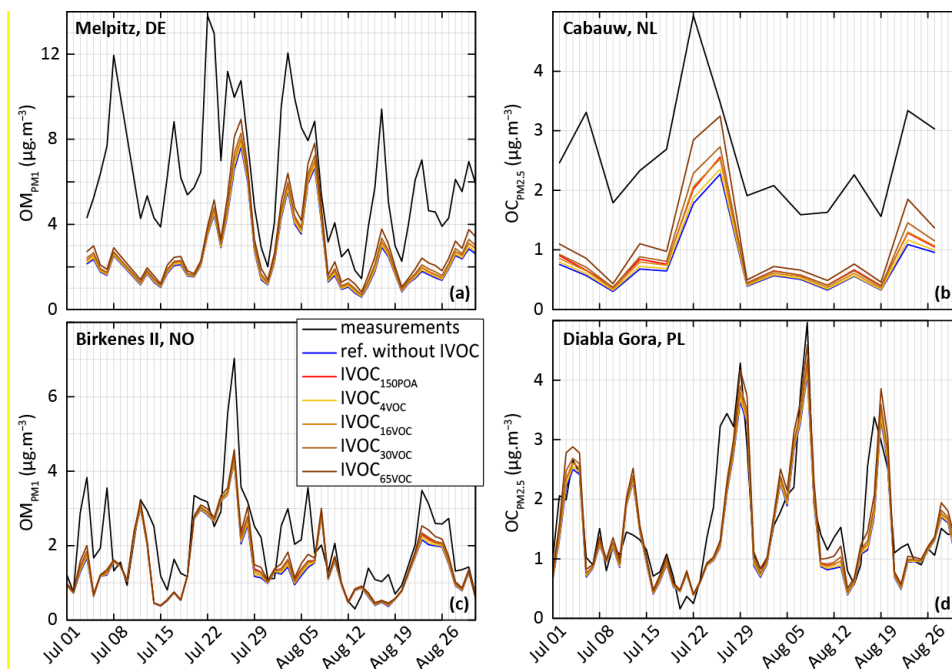
Figure 13 – Measured and simulated (for the ref-VBS-GECKO configuration without IVOC and the different model configuration considering IVOC emissions) temporal evolution of daily averaged OM_{PM1} concentrations (panels a and c) and $OC_{PM2.5}$ concentrations (panels b and d). Top panels are for stations close to anthropogenic sources in Germany (Melpitz station, a) and Netherland (Cabauw station, b) and bottom panels for stations in remote areas in Norway (Birkenes II station, c) and Poland (Diabla Gora station, d).

42
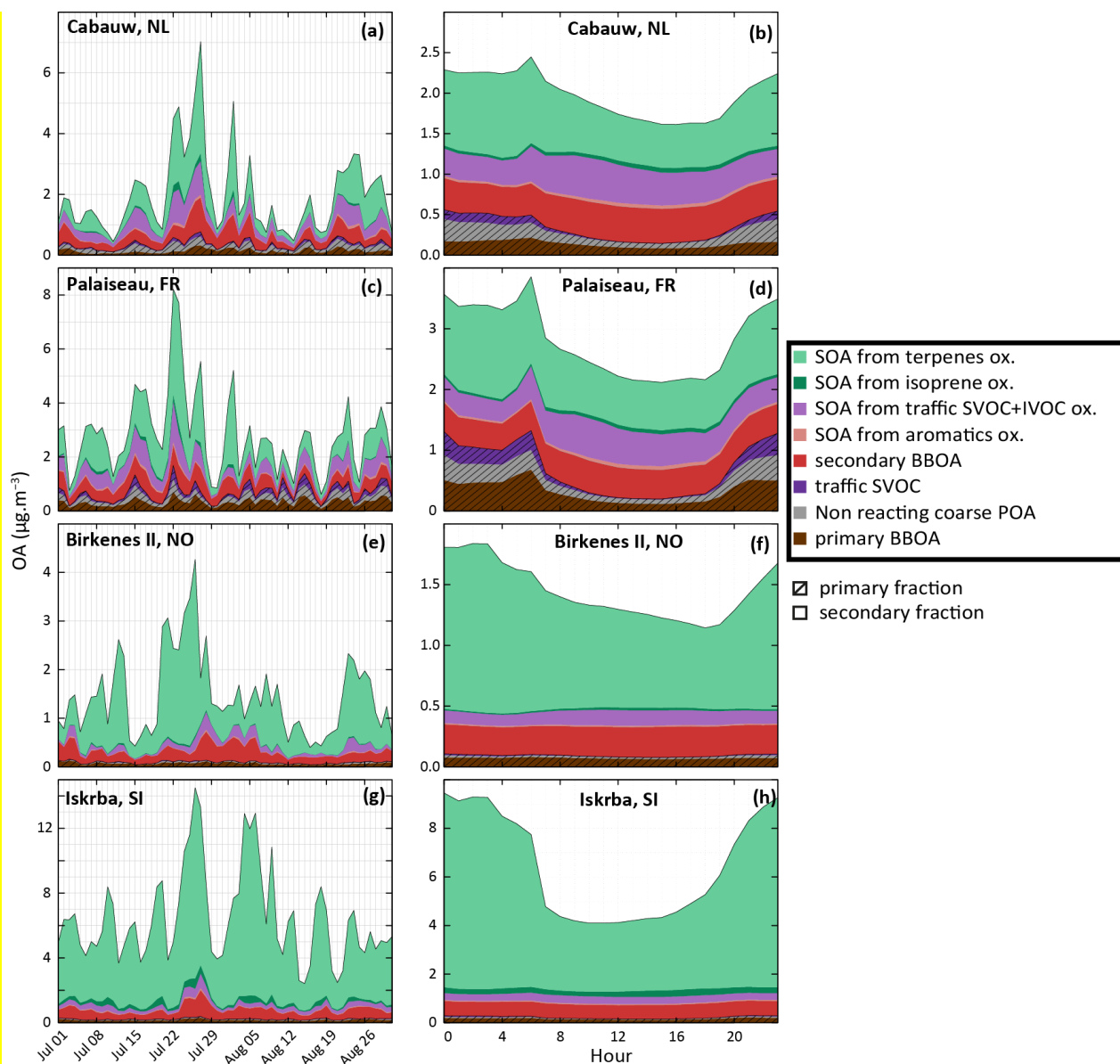
Figure 14 – Evolution of simulated OA concentrations and distribution function of sources with the IVOC$_{30VOC}$ model configuration. Panels a, c, e and g present evolutions of daily average concentrations during the July-August 2013. Panels b, d, f and h present mean daily profiles. Results are shown at two stations influenced by anthropogenic sources in Netherland (Cabauw, a and b) and in France (Palaiseau, c and d) and at two stations influenced by biogenic sources in Norway (Birkenes II, e and f) and Slovenia (Iskrba, g and h). Primary and secondary BBOA includes compounds from biomass burning. Traffic SVOC includes C$_{14}$ to C$_{26}$ VBS-GECKO alkanes and alkenes and SOA from traffic SVOC+IVOC oxidation includes their oxidation products. SOA from terpenes includes all species produced by α-pinene, β-pinene, limonene, ocimene and humulene oxidation.

Figure 15 – Mean simulated anthropogenic OA mass concentration formed by the partitioning of species produced from the oxidation of emitted traffic SVOCs (a), traffic IVOCs (b) and mono-aromatic compound (c) for July-August 2013 over Europe (data from IVOC$_{30VOC}$ simulation).

5